

Final Design Report



**University
of Manitoba** | **Price Faculty
of Engineering**

Horizontal Grain Aeration Testing and Measurement System

Submitted by:

BIOE4950 Team 8

Annika Wolfe, Mackdonald Maruhe, Mohamed Abosheloua, Stephane Le Heiget

For:

Dr. Fuji Jian and Harshini Boopathy

University of Manitoba

Advisors:

Dr. Natasha Jacobson, Dr. Don Petkau, Mr. James White, Ms. Aidan Topping

Department of Biosystems Engineering

University of Manitoba

Winnipeg, Manitoba, Canada

March 21, 2025

EXECUTIVE SUMMARY

Farmers around Canada, specifically in Manitoba, predominantly utilize vertical grain aeration in their post-harvest grain storage systems to extend the storage life of the grain. Using horizontal aeration presents a more energy-efficient alternative to vertical aeration. However, manufacturers lack the information and theoretical calculations necessary to optimize the design of horizontal aeration systems. This means that despite its advantages, manufacturers remain hesitant to adopt horizontal systems due to insufficient data to inform their design.

This project aimed to address this issue on behalf of Dr. Fuji Jian and the grain storage research group at the University of Manitoba. The project focused on creating a bench-scale device for testing and measuring air resistance in horizontal grain aeration systems. The device measures the performance of horizontal airflow through an aeration system that results from different types of grain and system configurations. Project deliverables included the constructed and verified device, and preliminary testing and data collection for future Ph.D. research and eventual industry application.

The project's technical specifications were verified to ensure that the final prototype would meet the client's demands for a grain bin that could hold a load of grain and measure the performance of horizontal grain aeration. A structural design was carried out to ensure that the grain bin could hold a whole load of grain during operation. Other verifications included testing the radial airflow uniformity, whether vertical airflow is negligible, and adapting the grain bin to be used with various system configurations. The grain bin was found to satisfy all the criteria required by the client. The overall project successfully provided a method to measure horizontal grain aeration performance from the data collected.

There are several recommendations for how to improve this project further. The main recommendation is to minimize instrumentation in the grain bin. A combination of pitot tubes and mass flow sensors were used to measure airflow. This combination provides highly detailed measurements, but the consequence is several disruptions to the airflow. Replacing or reducing the instrumentation disruption to the airflow would be reduced, producing higher quality results. Additionally, some operation procedure improvements are recommended to help future researchers transition to working with pilot-scale prototypes.

TABLE OF CONTENTS

EXECUTIVE SUMMARY.....	ii
LIST OF FIGURES	v
LIST OF TABLES	viii
1. INTRODUCTION.....	1
1.1. Grain Aeration and Horizontal Flow Overview	1
1.2. Existing Research on Horizontal Grain Aeration Systems.....	2
1.3. Implications and Eventual Client Goals.....	3
2. PROBLEM DEFINITION.....	4
2.1. Design Functions.....	4
2.2. Technical Specifications.....	5
2.3. Constraints.....	7
3. DESIGN SOLUTION.....	8
3.1. Major Subsystems	9
3.1.1. Octagonal Plenum.....	9
3.1.2. Perforated Bin.....	11
3.1.3. Airflow Measurement System	14
3.2. Operation and Data Collection Procedure.....	17
4. VERIFICATION PROCEDURES.....	21
4.1. Physical Size of Structure (S1.X).....	21
4.2. Physical Properties of Grain (S2.X).....	22
4.2.1. Size of Smallest Grain (S2.1)	22
4.2.2. Loading Capacity (S2.2).....	24
4.3. Instrumentation Specifications (S3.X).....	25

4.4. Airflow Properties (S4.X)	28
4.4.1. Airflow Direction (S4.1).....	28
4.4.2. Airflow Distribution (S4.2).....	28
4.5. Testing Operations (S5.X).....	30
4.5.1. Assembly Time (S5.1).....	30
4.5.2. Adjustability for Fans and Transitions (S5.2).....	30
4.5.3. Measurement Frequency and Test Length (S5.3, S5.4).....	31
5. SUSTAINABILITY.....	32
6. CONCLUSION	36
6.1. Project Limitations	36
6.2. Recommendations	38
REFERENCES	40
APPENDIX A: BILL OF MATERIALS.....	41
APPENDIX B: ENGINEERING DRAWINGS.....	46
APPENDIX C: ADDITIONAL INFORMATION ON SELECTED PARTS AND MATERIALS	65
APPENDIX D: FS7 CALIBRATION CALCULATIONS AND GRAPHS	78

LIST OF FIGURES

Figure 1. Potential air travel paths through the grain in the horizontal direction	2
Figure 2. Diagram of testing and measurement system device with color-coded subsystems.	8
Figure 3. Octagonal plenum with frame exposed (A) and fully assembled (B)	10
Figure 4. Image of ventilation subsystem	11
Figure 5. Concentric perforated columns and side door.	12
Figure 6. Side door assembly.....	13
Figure 7. Flowchart of mass flow sensor system.....	14
Figure 8. Data acquisition system with from, left to right, enclosure for the evaluation boards, power supply, and data acquisition system.	15
Figure 9. Pitot support frame with pitot tubes installed.....	16
Figure 10. Calibration materials pictured left to right: desktop fan; sensor and 3D printed holder (pink) on calibration mount under plastic box; power supply.	26
Figure 11. Sample calibration graph for mass flow sensor.	27
Figure B1. Detailed engineering drawing of the solid square bar-1	47
Figure B2. Detailed engineering drawing of the solid square bar-2.	48
Figure B3. Detailed engineering drawing of the diamond metal mesh.	49
Figure B4. Detailed engineering drawing of the square bar assembly.	50
Figure B5. Detailed engineering drawing of the flat top support bar.	51
Figure B6. Detailed engineering drawing of the full subsystem assembly showing placement of the diamond metal mesh, flat top support bar.	52
Figure B7. Detailed engineering drawing of the plenum base.....	53
Figure B8. Detailed engineering drawing of the plenum top.....	54
Figure B9. Detailed engineering drawing of the external ring cuts.....	55
Figure B10. Detailed engineering drawing of Internal ring cuts.	56

Figure B11. Detailed engineering drawing of the vertical supports.	57
Figure B12. Detailed Engineering drawing of the Cross Beam Supports.	58
Figure B13. Detailed engineering drawings of the full plenum subassembly	59
Figure B14. Detailed engineering drawings of the discharge chute on the side door.....	60
Figure B15. Detailed engineering drawings of the side support on the side door.	61
Figure B16. Detailed engineering drawing of 3D printed sensor mount assembly.	62
Figure B17. Detailed engineering drawing of 3D printed sensor holder.	63
Figure B18. Detailed engineering drawing of 3D printed beam holder.....	64
Figure C1. Dimensions of the perforation on the steel sheet metal.	68
Figure C2. Free body diagram and calculation of forces acting at fixed supports (welded) A and B.....	70
Figure C3. Diagram of the Shear force diagram (SFD) and Bending Moment diagram indicating the maximum shear force and bending moment acting on a 0.375in X 0.375in solid square steel bar.....	70
Figure C4. Specifications for Northern Blower fan used for testing.	72
Figure C5. Manufacturer specifications for iST FS7 thermal mass flow sensors.....	73
Figure C6. Manufacturer specifications for Dwyer pitot tubes	74
Figure C7. Manufacturer specifications for KANOMAX Anemomaster A031 hot wire anemometer.....	75
Figure C8. Manufacturer specifications for REED R3030 digital manometer.....	76
Figure C9. Manufacturer specifications for REED R3030 digital manometer.....	77
Figure D1. Calibration graph and calculated parameters for sensor A.	79
Figure D2. Calibration graph and calculated parameters for sensor K.....	80
Figure D3. Calibration graph and calculated parameters for sensor C.	81
Figure D4. Calibration graph and calculated parameters for sensor L.	82

Figure D5. Calibration graph and calculated parameters for sensor E.	83
Figure D6. Calibration graph and calculated parameters for sensor F.	84
Figure D7. Calibration graph and calculated parameters for sensor G.	85
Figure D8. Calibration graph and calculated parameters for sensor H.	86
Figure D9. Calibration graph and calculated parameters for sensor I.	87
Figure D10. Calibration graph and calculated parameters for sensor J.	88

LIST OF TABLES

TABLE 1. LIST OF TECHNICAL SPECIFICATIONS.....	5
TABLE 2. LIST OF PROJECT CONSTRAINTS AND LIMITATIONS	7
TABLE 3. DATA COLLECTION PROCEDURE	17
TABLE 4. SYSTEM OUTPUTS AND OUTPUT DATA TYPES.....	19
TABLE 5. SYSTEM INPUTS AND SELECTED INPUT PARAMETERS	20
TABLE 6. S1.1-S1.4 VERIFICATION RESULTS.....	21
TABLE 7. SIEVE ANALYSIS DATA	23
TABLE 8. S2.1 VERIFICATION RESULTS	24
TABLE 9. S2.2 VERIFICATION RESULTS	25
TABLE 10. S4.1 VERIFICATION RESULTS	28
TABLE 11. S4.2 VERIFICATION RESULTS	29
TABLE 12. S5.1 VERIFICATION RESULTS	30
TABLE 13. S5.2 VERIFICATION RESULTS	31
TABLE 14. GPM SUSTAINABILITY ANALYSIS.....	32
TABLE A1. BILL OF MATERIALS	41
TABLE C1. RESULTS OBTAINED FROM STRUCTURAL ANALYSIS OF BIN WALL.....	66
TABLE C2. PROPERTIES OF PERFORATED SHEET METAL.....	67

1. INTRODUCTION

In Manitoba, post-harvest grain is loaded into storage bins, often at high temperatures and moisture levels, creating an environment prone to pests and spoilage. Aeration systems in grain bins are implemented to counteract this by pushing ambient air through the bulk to cool and dry it while in storage. This method is known as ambient drying and is commonly done by pushing the air vertically through the grain mass. Horizontal flow through grain storage bins can be an alternative to vertical flow. Research shows that the static pressure within the media opposing air movement can be reduced by 30-60% when the air flows horizontally instead of vertically [1]. Lowering the pressure an aeration system must work against can reduce energy costs and drying times for farmers. However, there is a lack of available literature for manufacturers on designing these systems and their optimal function.

Dr. Fuji Jian, P.Eng., is an Associate Professor in the Department of Biosystems Engineering at the University of Manitoba, whose research focuses on improving the handling and storage of post-harvest grain. He has been contacted by several industry members seeking guidance on the design of horizontal aeration systems. Under the instruction of Dr. Jian, this project produced a bench-scale horizontal flow grain aeration system that can be manipulated to test its performance under changing parameters. The device was designed to be compatible with future graduate and doctoral research to address the existing data gaps.

1.1. Grain Aeration and Horizontal Flow Overview

The primary goals of post-harvest grain aeration are to cool and dry the grain once it is loaded into the bin. Regulating temperature and moisture levels within the grain bulk can prevent unwanted moisture accumulation, the formation of hot spots, crop spoilage, and the survival of pests. Farmers may also aim to achieve or maintain a specific moisture level in the crop in preparation for sale or storing the grain for longer-term purposes [2]. Ambient drying in grain bins is convenient as it comes at a low energy and capital cost to farmers.

An aeration system must successfully overcome the static pressure resisting the fan to push air through the grain bulk. This static pressure is the frictional resistance from the airflow through the grain bulk, air distribution system, and the transitional duct connecting the fan [3].

Many factors influence the static pressure exerted by the grain bulk: the type of crop, porosity, the shape of the pores within the media, depth of the grain bed, grain moisture content, and velocity and direction of airflow through the bulk [1].

Studies have shown that airflow direction through the grain bulk can significantly affect the airflow resistance. Airflow resistance through a grain bulk in the horizontal direction is generally lower than in the vertical direction, though no singular rule has been developed. Horizontal airflow resistances are reported as between 0.4-0.7 times that of vertical resistance [1]. X-ray CT analyses of grain bulks have shown that the area and length of spaces through which air can travel are 30% to 100% higher in the horizontal direction than in the vertical direction, depending on the crop type [4]. Figure 1 below shows how air may travel horizontally through a grain bulk over a length L and a pressure difference of P_2-P_1 .



Figure 1. Potential air travel paths through the grain in the horizontal direction. Adapted from [1]

The hypothetical air streams around the grain kernels shown in Figure 1 have a more direct path of travel than if they had been oriented vertically. This path can be attributed to the grain kernels' shape and packing orientation. Kernels will tend to fall with their long axis horizontally [5], creating a path of greater tortuosity for air travel in the vertical direction as opposed to the horizontal.

1.2. Existing Research on Horizontal Grain Aeration Systems

While the potential advantages of horizontal flow systems are well-established, considerably less research has been conducted on the design and performance of systems that utilize this concept. The few existing studies demonstrate that changing a single parameter

significantly impacts the system's performance. One study evaluating a horizontal flow system proved that wheat dried radially from the centre when air was pushed into the bulk from a central column and vented through the bin sides [6]. The results showed that the airflow was distributed uniformly throughout the radius of the bulk and that a consistent pressure throughout the height could be achieved given the correct central column height. However, the system proved ineffective if the column height was too short [6].

In [7], a computational model was developed that accounted for the changes in pore structure that a grain bulk experiences due to compaction under its weight. Differences in air velocity up to 84% through the vertical depth were observed using a model of a flat-bottom grain storage bin equipped with a horizontal flow system [7]. The results suggested that a lack of effective aeration may occur in the lowest layers of the grain in commercial-sized systems due to compaction without proper design considerations [7].

A 2024 study investigated horizontal airflow through a 50 cm cube of wheat containing various levels of dockage [8]. Dockage - any waste or particle in the bulk other than the grain - is present in all post-harvest grain in some measure. The study found that resistance to horizontal airflow could be significantly impacted by the presence and distribution of dockage in the grain bulk [8].

All three of these studies demonstrate the need for continual research and the improvement of horizontal aeration system designs, given the broad scope of parameters that influence airflow resistance and the fact that they vary from case to case. The advantages of horizontal airflow can only be utilized if it is understood how the systems respond to different variables in a commercial environment.

1.3. Implications and Eventual Client Goals

This capstone project is part of a larger initiative, which aims to provide manufacturers with usable data to optimize the design of horizontal aeration systems. The results from this project will be incorporated into future Ph.D. research, with the eventual goal of using the collected data to build a mathematical model predicting the effects of manipulating different variables within the system. The project is designed to allow for further testing of different

combinations of fans, transitions, grain types, internal column sizes, inlet surface areas, and outlet areas. The constructed device will provide the physical measurements used to validate the Ph.D. student's calculated values from the model and serve as a bench-scale prototype of a future full-scale testing system. This project is a step towards filling in some observed data gaps and help guide manufacturers' decision-making.

2. PROBLEM DEFINITION

The client, Dr. Jian, required an airflow measurement system to measure air resistance when horizontal airflow is applied in a grain bulk using different ventilation systems. The goal of this design was to produce a device that measures 2D horizontal airflow through the grain.

Project deliverables include the constructed and verified device, which consists of a functioning measurement system and structural components, a complete bill of materials (Appendix A), and engineering drawings for the structural components of the design (Appendix B).

2.1. Design Functions

The design must fulfill the following functions:

- Measure air resistance and airflow when the grain is ventilated using a horizontal flow ventilation system.
- Ensure that horizontal airflow is achieved through the grain, and vertical airflow is minimized.
- Ensure that airflow is radially uniform so that the grain is equally ventilated.
- Consist of a metal cylindrical bin on top of a plenum.
- Be approximately 2 meters in diameter to accommodate future testing.
- Use a perforated column as the air inlet in the center of the grain bulk and vent out of the sides of the bin.
- Support the weight of the grain when full.
- Be able to test different surface areas of perforation on the inlet column.
- Be adjustable for different configurations of fans and transitions.

- Accommodate different sizes of grains ranging from small seeds like canola (1.6 mm in diameter) to larger seeds like peas (2.5 mm in diameter) and irregular-sized seeds like corn (7.36 mm x 6.29 mm).
- Take at most 4 hours to reconfigure the ventilation system.
- Allow for efficient loading and unloading of grain without damage to any components.

These functions are essential for the design to meet the client's requirements. Failure to meet these functions results in the design failing to achieve the client's desired tasks.

2.2. Technical Specifications

The technical specifications of the project are listed in Table 1. Specifications S1.X are the physical dimensions of the design, specifications S2.X are the physical properties of the grain, S3.X are the specifications related to the instrumentation utilized in the design, and S4.X are the airflow properties, and S5.X are specifications for the assembly and testing operations.

TABLE 1. LIST OF TECHNICAL SPECIFICATIONS

Spec. #	Definition	Criteria	Verification Procedure
Physical Size of Structure			
S1.1	Height of bin	1470 ± 50 mm	4.1
S1.2	Diameter of bin	1920 ± 50 mm	4.1
S1.3	Height of internal column	≤ 610 mm	4.1
S1.4	Diameter of internal column	380 - 500 mm	4.1
Physical Properties of Grain			
S2.1	Size of the smallest grain	Canola seed	4.2.1
S2.2	Load capacity	5000 kg	4.2.2
Instrumentation Specifications			
S3.1	Manometer pressure measurement range	0-206.8 kPa	4.3

TABLE 1. LIST OF TECHNICAL SPECIFICATIONS - CONTINUED

Spec. #	Definition	Criteria	Verification Procedure
S3.2	Resolution and accuracy of manometer measurements	0.2 kPa; 0.3% of full scale at 25°C	4.3
S3.3	Hot wire anemometer velocity measurement range	0.10 m/s to 30.0 m/s	4.3
S3.4	Resolution and accuracy of hot wire anemometer measurements	0.01 m/s at 0.00 m/s to 9.99 m/s; \pm (3% of the reading +0.1) m/s	4.3
S3.5	Mass flow sensor velocity measurement range	0 m/s to 100 m/s	4.3
S3.6	Resolution and accuracy of mass flow sensor measurements	0.01 m/s; <3% of measured value	4.3
S3.7	Fan specifications	110 CFM; 6" S.P.; 3200 rpm	4.3
Airflow Properties			
S4.1	Vertical airflow is minimized	0 m/s through top of grain	4.4.1
S4.2	Radial airflow uniformity	Maximum \pm 10% variation from the mean	4.4.2
Testing Operations			
S5.1	Maximum time for assembly	< 4 hours	4.5.1
S5.2	Accommodates multiple fans and transitions	Secure fit; No air leakage	4.5.2
S5.3	Frequency of measurements	30 seconds	4.5.3
S5.4	Duration of test	15 minutes	4.5.3

In Table 1, S1.1 and S1.2 are the fixed values of the bin. Specifications S1.3 and S1.4 are the physical size of the perforated column used, with the height of the column being determined according to recommendations from Chelladurai [6]. Based on discussions with the client, the

smallest grain that will be used with the airflow unit is canola, which is why S2.1 was chosen. S2.2 was chosen based on the bulk density of wheat, which has the highest bulk density of all potential grains, multiplied by the bin volume with a factor of safety of 1.5 and then rounded to the nearest hundred. S3.1 to S3.7 represent the specifications of the instrumentation utilized in the design. These are found in the individual product specification sheets located in Appendix C. Specifications S4.1 and S4.2 define the requirements for the airflow to be primarily horizontal and radially uniform. This ensures that the 2D airflow shown in Figure 2 can be used to determine 3D airflow by projecting it radially. S5.1 to S5.4 are performance specifications provided by the client that the design must meet.

2.3. Constraints

The project has several constraints and limitations guiding the design and functionality of the final device. Table 2 shows the descriptions and implications of the constraints.

TABLE 2. LIST OF PROJECT CONSTRAINTS AND LIMITATIONS

Constraint #	Description	Mitigation Strategy
C1	The project budget is limited to approximately \$5000, with additional expenses requiring approval	All purchases will be made through and approved by Dr. Jian, the Biosystems office, and/or Agriculture and Agri-Food Canada.
C2	Predetermined components provided by Dr. Jian.	Parts provided include a transition fan connection, a Northern Blower 7993 size 6 centrifugal fan, and an internal cylindrical perforated column with a lid.
C3	The project is less than 7 months long, beginning in mid-September 2024 and ending in March 2025.	The scope of testing is limited to accommodate the timeframe. Project progress is tracked with a regularly updated Gantt chart.

3. DESIGN SOLUTION

There are three major subsystems to the design: (1) a plenum and attached ventilation subassembly, (2) a perforated bin with an internal column, and (3) an airflow measurement system. Figure 2 shows the assembly of the three systems and the air travel path through the device.

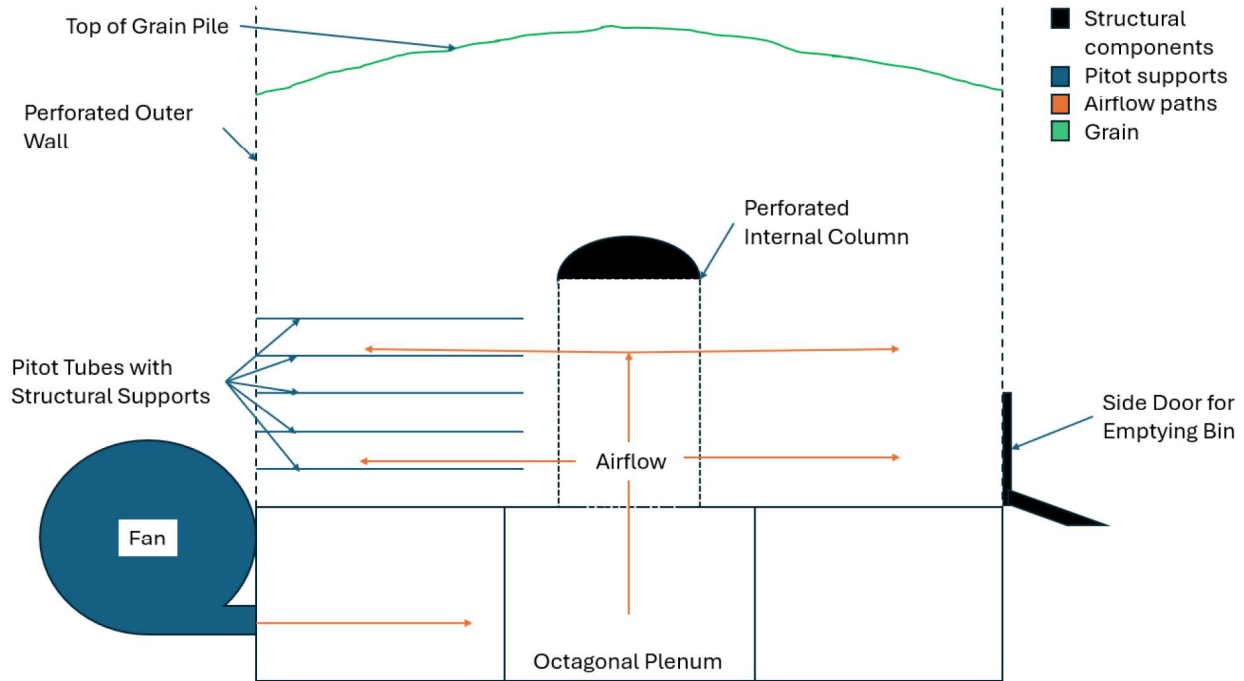


Figure 2. Diagram of testing and measurement system device with color-coded subsystems.

The design functions by moving air from a fan through a transition and into the plenum base. The plenum is connected to a perforated internal column, which vents the air horizontally into the bin. Then, the air is ventilated through a perforated exterior wall. The air is forced to travel horizontally through the grain due to the static air pressure exerted by the grain above the top of the internal column. A system of thermal mass flow sensors, pitot tubes, and a hot wire anemometer measure airflow property through the grain bulk. This produces a comprehensive testing and measurement system.

3.1. Major Subsystems

The three major subsystems and their relevant subassemblies are outlined in detail below. The systems are intended to be adaptable and scalable for modelling purposes. Material selection prioritized readily accessible and low-cost options to provide flexibility in future study applications. Engineering drawings for the systems can be found in Appendix B and a complete bill of materials is found in Appendix A.

3.1.1. Octagonal Plenum

The first subsystem is the octagonal plenum and attached ventilation subassembly. The plenum, shown in Figure 3, serves as the structural foundation for the grain bin. It provides a solid foundation for the bin and contains lateral support for the bin walls. The plenum has the following specifications:

- Plenum Dimensions: octagonal with a width of 1.98 m and a height of 0.3 m
- Lumber frame made from 2"x4" lumber for structural support
- Sheathed with 11 mm (7/16") plywood and sealed using silicone caulking
- FOS of 8.6, with a design load of 970 Pa and a failure load of 8.3 MPa

The lumber frame provides structural support allowing for the plenum to hold the load of the grain, and it is sheathed with plywood with all the joints sealed with silicone caulking to prevent air escaping into the external environment. The plenum has a hole on one side that allows the fan transition to attach, and a hole on the top surface of it to allow air to move up and into the bin above. The factor of safety of 8.6 is based on the structural design calculations, the heavy-duty lumber frame means that the plenum is overdesigned for the load. This is due to the use of 2"x4" lumber since that is a standard size carried by all lumber supply stores which made it readily available. Using 2"x4" lumber allowed the interior and exterior rings to be easily constructed and made it simple to seal using plywood and silicone, while also providing structural support for the internal column and sensor mounts.



(A)

(B)

Figure 3. Octagonal plenum with frame exposed (A) and fully assembled (B)

The ventilation subassembly, which includes the fan, transition, and an airflow rate control, is attached to the exterior of the octagonal plenum to supply aeration for the unit. It transitions from the fan into the plenum, where the air is forced upward into the internal column placed inside the grain bulk. The fan selected for the ventilation assembly determines the pressure generated at specific air flows. The fan is connected to a duct, composed of transitions to connect the fan to the plenum and with a ball valve, as shown in Figure 4. Adjusting the valve will control the airflow rate that will flow into the plenum. No instrumentation was installed to measure airflow before entering the plenum, as it was outside the scope of this project.

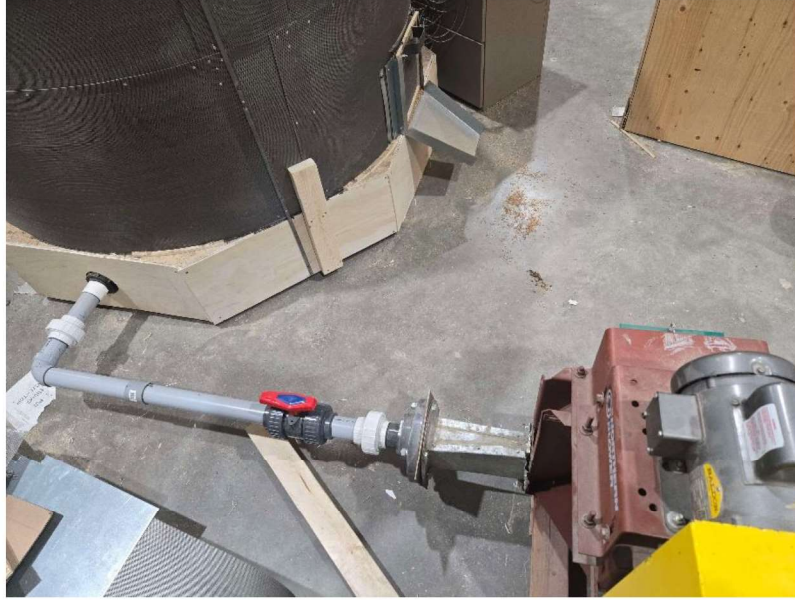


Figure 4. Image of ventilation subsystem

The valve allows for a convenient way to change the airflow rate and apply different airflow velocities. Measurements of airflow at different rates can be used to create future fan charts, which are essential to designing grain aeration systems. This adjustable airflow rate will optimize future designs and further research into horizontal airflow based on the performance metrics collected using the measurement subsystem.

3.1.2. Perforated Bin

The second main component is the cylindrical grain bin, shown in Figure 5. The bin is designed to form a horizontal airflow through the grain when air is supplied. The exterior perforated wall is the outlet for the grain aeration system, while the internal perforated column serves as the airflow inlet. Additionally, the outer wall must structurally support the lateral pressure of the grain applied by the bulk when the bin is filled.



Figure 5. Concentric perforated columns and side door.

The outer wall of the bin is built out of 20-gauge metal sheets with 1.57 mm (0.062") diameter perforations and 40% open surface area. The outer column has a total height of 1.72 m and is made of several riveted perforated metal sheets to form a 1.92 m diameter rigid cylinder. The wall is reinforced with 3.2mm x 6.4mm (1/8"x1/4") steel bars bolted to the plenum to account for the lateral pressures applied onto the column from the depth of the grain. This support also holds the outer column firmly in place during testing. Pressure calculations can be found in Appendix C. Using a perforated outer wall provides complete control over the configuration of external venting. The exposed perforated surface area is adjustable by affixing plastic sheeting over any section of the bin wall.

The internal column is a prefabricated perforated column, through which air is supplied to the grain. For the verification procedures, an inner column with a 380 mm diameter and a height of 610 mm was selected. The internal column sits above the hole in the top of the plenum, which is covered by the same perforated sheet metal as the bin wall. This allows internal columns with different diameters to be used in testing without having to change the size of the center hole. The column is held in place by the pressure of the grain during testing. Any perforated surface area outside the diameter of the internal column is covered in plastic to

prevent air from entering the bottom of the grain bulk, ensuring the airflow is purely horizontal. This creates a radially uniform horizontal airflow that travels through the grain bulk until it exits it through the external perforated column.

Additionally, the internal column has a prefabricated conical lid to enclose it and prevent grain from entering. It also provides structural support by distributing and supporting the weight of the grain above the internal column. Adjustments can be made to the column's exposed surface area by detaching the lid and placing plastic sheeting inside the column. The lid secures the plastic from the top while the airflow holds it flush against the column's interior while in operation.

Once assembled, the bin can either be filled using a grain auger from the top or filled by hand. One side door has been placed on the external bin wall to empty the grain inside the bin into a grain auger after testing is complete. A diamond mesh was installed over the opening to provide structural support as well as prevent any instrumentation that may have become loose during operation from entering the auger. The side door assembly is shown in Figure 6.



Figure 6. Side door assembly.

The side door is made of the same perforated metal as the bin walls, sits in a wood frame, and is held in place by brackets made from galvanized sheet metal. A handle is used to lift and lower the door, allowing for the bin to be emptied after testing is complete. Finally, a grain

discharge chute made of galvanized sheet metal is attached to the base of the door frame. The discharge chute directs the grain flow so that grain falls into the hopper of the auger, and spillage can be minimized.

3.1.3. Airflow Measurement System

Airflow velocity is measured as it moves through the internal column before it enters the grain bulk. Two sets of five thermal mass flow sensors are installed to measure the vertical velocity through the column. The sensors are aligned horizontally with the pitot tubes and secured by 3D printed mounts onto vertical support bars. The first set is fixed in the center of the internal column, while the second set is placed near the column wall.

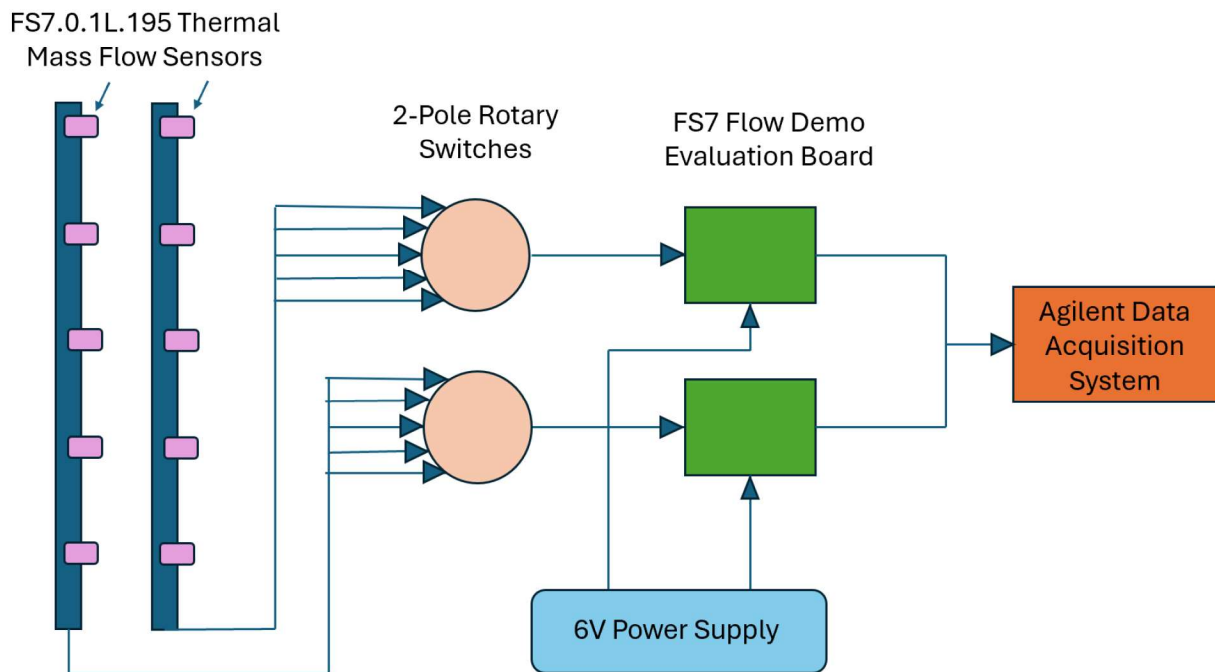


Figure 7. Flowchart of mass flow sensor system.

Each set of five sensors is connected to a 2-pole rotary switch, which is then connected to a respective evaluation board. The switches allow one sensor from each set to be transmitting a signal to the board at a time. The two evaluation boards require an input of 6-9 V, provided by the power supply shown in Figure 8. The sensors are calibrated to correlate the voltage output to an airflow velocity. The output is read by an Agilent data acquisition system connected to the

evaluation boards. A bench calibration was performed on each sensor for a range of 0 m/s to 6.4 m/s. Sensor calibration data and equations are included in Appendix D.

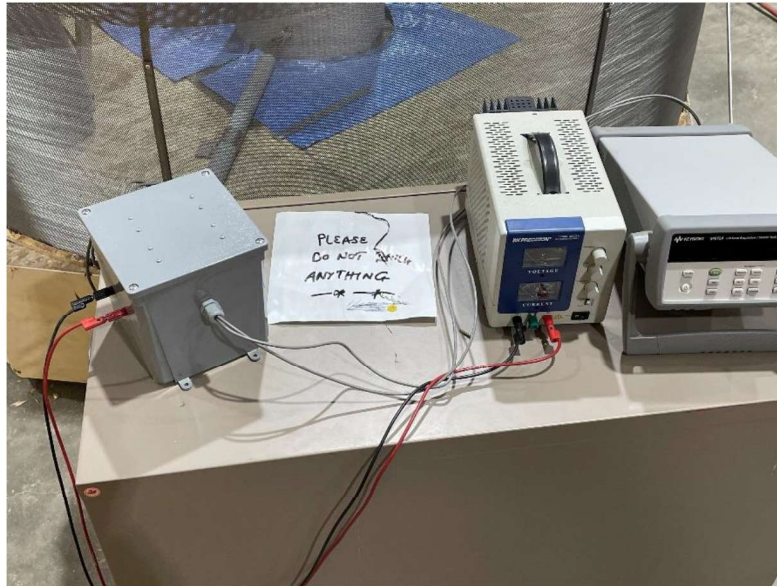


Figure 8. Data acquisition system with from, left to right, enclosure for the evaluation boards, power supply, and data acquisition system.

Within the grain bulk, two sets of five pitot tubes were used to measure air pressure in a 2D plane. The first set is located after the air enters the grain from the inlet, and the second set is before the air exits the bin. A custom-built metal frame was made to provide structural support to the pitot tubes. The frame was built using diamond meshes welded to 9.5 mm (3/8") square bars as shown in Figure 9. The 9.5 mm (3/8") square bars had a FOS of 4.0, full design calculations can be found in Appendix C. It was decided to overdesign the metal support frame so that assembly would be easier as any square bars below 9.5 mm (3/8") become more challenging to weld due to their smaller size.



Figure 9. Pitot support frame with pitot tubes installed.

As shown in Figure 9, the pitot tubes are attached to the custom-built metal frame and zip tied into position. These supports ensure that the pitot tubes stay in place during testing to prevent errors in the results. The first set of pitot tubes measure the pressure after the air exits the internal column and are placed 300 mm away from the center of the bin. This placement allows for an internal column with a diameter of up to 500 mm. The second set of pitot tubes measure the pressure drop before the air exits the external column and are placed 150 mm from the external wall to reduce the effect of the instruments on airflow exiting the bin. The pitot tubes are installed in five layers with 90 mm of vertical spacing, starting from 25 mm above the floor of the bin. There are five pitot tubes with a 7.9 mm (5/16") diameter and 6.25 m (24-5/8") insertion length and five with a 7.9 mm (5/16") diameter and 9.30 m (36-5/8") insertion length.

Pressure readings from the pitot tubes are taken by two digital manometers, so both values in a single horizontal plane can be read simultaneously. The manometer used was a Reed R3030. The airflow exiting the grain bulk through the external column is manually measured outside the bin using a hot wire anemometer. The hot wire anemometer is a Kanomax A301 hot wire anemometer. The specifications for the equipment of the instrumentation can be found in Section 2.2 under Table 1.

3.2. Operation and Data Collection Procedure

A procedure for operating the device and collecting data during testing was developed and is detailed below. It was designed to comply with this project's time and budget constraints while considering the device's future uses and user needs.

TABLE 3. DATA COLLECTION PROCEDURE

Step #	Item	Action
1	System assembly	<ul style="list-style-type: none">• Place the internal column in the center of the bin above the hole in the plenum.• Use plastic sheeting to prevent airflow through any undesired perforated surface area. This includes adjusting the exposed surface area on the internal column, the external bin wall, and any perforation on the bin floor not covered by the internal column.• Connect the fan transition to the plenum through the connection port in the plenum's side.
2	Grain loading	<ul style="list-style-type: none">• Load grain into the bin with augers or by hand.• Evenly distribute grain once bin is fully filled.
3	Start test	<ul style="list-style-type: none">• Adjust valve on transition as required.• Turn on fan.
4	Velocity and pressure data recording	<ul style="list-style-type: none">• Turn on power supply to mass flow sensor evaluation boards and data acquisition system.• Set mass flow sensor switches to settings A and F, corresponding to the top sensor in each set. Each set is connected to a channel in the data acquisition system. The data system will display the voltage reading from one channel at a time but can switch between the two instantaneously.

TABLE 3. DATA COLLECTION PROCEDURE - CONTINUED

Step #	Item	Action
4	Velocity and pressure data recording - continued	<ul style="list-style-type: none"> • Record following data simultaneously for a single horizontal plane. This includes one mass flow sensor from each set, two pitot tubes, and an exit velocity reading. <ul style="list-style-type: none"> ○ Read the voltage from both channels of the data acquisition system every 30 seconds for 15 minutes. ○ Record pressure output measurements every 30 seconds for 15 minutes using two manometers, one connected to each pitot tube. ○ Record outlet air velocity every 30 seconds for 15 minutes using a hot wire anemometer. If the exit velocity is below the threshold of the anemometer, a large cone with a gradual contraction can increase the velocity outside of the bin wall. The average exit velocity over the area is related by flow continuity. • Switch manometers to pitot tubes on next horizontal plane. Turn mass flow sensor switches to next stop, (A and F, B and G, etc.). • Repeat for all five horizontal planes.
5	End test	<ul style="list-style-type: none"> • Turn off fan.
6	Grain emptying	<ul style="list-style-type: none"> • Open exit door and allow the grain to flow out of the bin under gravity. • Remove any remaining grain with a vacuum

The measurement system uses instrumentation that produces five separate outputs values to be used in analysis. Each instrument is listed in Table 4 in the order which it is passed by air moving through the system. The respective data type and how that data is obtained is indicated in the right-hand column.

TABLE 4. SYSTEM OUTPUTS AND OUTPUT DATA TYPES

#	Output	Data Obtained for Analysis
1	Thermal mass flow sensor	Output voltage read by data acquisition system correlated to airflow velocity
2	Thermal mass flow sensor	
3	Pitot tube	Manual pressure readings from a manometer
4	Pitot tube	
5	Hot wire anemometer	Manual airflow velocity readings

Data is analyzed by converting all velocity measurements to pressure values (outputs 1, 2, and 5). Pressure drops between instruments across each horizontal plane can be compared to determine the loss experienced from passing through the internal column, grain bulk, or external column. Pressure drops across the horizontal plane can also be compared to one another to analyze the vertical uniformity of the airflow and how the airflow is affected by depth. Finally, data sets can be compared between test treatments with changing input variables to look at the effect of different ventilation systems.

There are five variables that can be adjusted in the design to obtain and compare output data. These input variables are listed in the table below. The selected input parameters used in the scope of this project to test and verify the function of the design are listed accordingly. Tests were conducted using the procedure outlined in Table 3.

TABLE 5. SYSTEM INPUTS AND SELECTED INPUT PARAMETERS

#	Input	Selected Input Parameters
1	Grain type	Wheat
2	Internal column dimensions	Diameter: 380 mm; Height: 610 mm
3	Percent of internal column perforated surface area exposed	100%
4	Percent of external column perforated surface area exposed	100%
5	Fan and transition configuration	Northern Blower 7993 size 6 centrifugal fan, Transition valves 100% open

The technical specifications in Table 1 indicate the allowable ranges for input parameters 1 and 2 (S1.3, S1.4, and S2.1). The description of each subsystem shows how the design accommodates changing each input variable. Adjustability for these inputs is a key design function and is what ensures the device meets the client’s needs and future goals for the project.

4. VERIFICATION PROCEDURES

The procedures below verify the technical specifications outlined in Table 1. Each procedure is listed with its corresponding specification. Pass/fail criteria and justifications are included where necessary.

4.1. Physical Size of Structure (S1.X)

Specifications S1.1, S1.2, S1.3, and S1.4 refer to the physical size of the design. These specifications were verified by measurement with a measuring tape. The design is considered adequate if the horizontal air travel path is less than or equal to 130% of the shortest potential vertical air travel path. This specification is based on the lower limit of the observed horizontal versus vertical pressure differences described in [1]. Therefore, pass/fail of the criteria is governed by:

$$\frac{S1.2 - S1.4}{2} \leq (S1.1 - S1.3) * 1.30$$

S1.1 and S1.2 have a target value of within 5 cm of their specified measurements to provide a margin for manufacturing variability. S1.3 and S1.4 are measurements of the prefabricated internal perforated column and are a pass if they comply with the above constraints. S1.3 is measured from the base of the column to the bottom of the lid. S1.4 is the external diameter of the column. The following dimensions were obtained from the fully assembled device:

TABLE 6. S1.1-S1.4 VERIFICATION RESULTS

#	Item	Target	Measured	Satisfied (Y/N)
S1.1	Bin height	1470 ± 50 mm	1422 mm	Yes
S1.2	Bin diameter	1920 ± 50 mm	1960 mm	Yes
S1.3	Internal column height	610 mm	610 mm	Yes
S1.4	Internal column diameter	380 - 500 mm	380 mm	Yes

Inputting the measured values into EQN (1) yields:

$$\frac{1960 - 380}{2} \leq (1422 - 610) * 1.30$$
$$790 \leq 1055.6$$

The equation is satisfied under the given measurements, therefore specifications S1.1-S1.4 pass their criterion.

4.2. Physical Properties of Grain (S2.X)

Specifications S2.1 and S2.2 refer to the device's compatibility with the physical properties of the grains used in its operation.

4.2.1. Size of Smallest Grain (S2.1)

The smallest grain size compatible with the device is determined by the perforation size in the outer bin wall. Availability of off-the-shelf perforated metals limited the minimum perforation diameter that could be obtained within the timeframe and budget of the project. The diameter of the perforations in the bin wall are 0.062-inches or approximately 1.57 mm. Therefore, the design is compatible with any seeds having a minor diameter greater than 1.57 mm.

At the client's request, the smallest design grain is canola seed and further testing was performed to determine its compatibility with the design. Variability in the diameter of canola seeds is expected and can be dependent on where it was purchased from and when. Therefore, S2.1 was verified based on the size distribution of canola seed available at the time of this project in the on-campus lab. An initial target of a maximum 15% (by mass) of the seeds falling below the perforation size was set as the passing criteria. A seed diameter distribution of selected sizes was determined by performing a sieve analysis, adapted from ASABE standard ANSI/ASAE S319.5 "Method of Determining and Expressing Fineness of Feed Materials by Sieving [9]." The test procedure is outlined below:

Sieve Analysis Procedure for Determining Distribution of Selected Seed Diameters:

Materials and equipment: Canola seed, container, scale with precision to 0.1 grams, Retsch sieve shaker, Retsch woven wire-cloth sieves (US sizes 10, 12, and 14)

Procedure:

1. A mass of 893.5 grams of canola seed was obtained from the grain storage lab and weighed.
2. The seeds were transferred to a Retsch sieve shaker equipped with a set of woven wire-cloth sieves. Sieve sizes 10, 12, and 14 were used, corresponding to aperture sizes of 2.0 mm, 1.70 mm, and 1.18 mm, respectively. (Note that all seeds were greater than 1.18 mm.)
3. The sieves were agitated at a speed of 175 rpm for 10 minutes.
4. The portion of seeds remaining in each sieve were removed and then weighed. Using the total mass, the proportion of seeds falling in each size range was determined.

The results from the sieve analysis are summarized in the table below.

TABLE 7. SIEVE ANALYSIS DATA

Initial Mass	Mass ≥2.0 mm	Mass ≥1.70 mm	Mass <1.70 mm	Proportion <1.70 mm
893.5 g	6.2 g	683.9 g	203.4 g	0.228

Since there is no sieve aperture size between 1.18 mm and 1.70 mm, the procedure above overestimates the true proportion of seeds falling below 1.57 mm in diameter. This limited the confidence with which the initial passing criteria could be verified, as the shape of the seed distribution below 1.70 mm and the minimum seed diameter were unknown. Assuming that <1% of the seeds fell below 1.20 mm and that the seed diameters follow a normal population distribution, the estimated proportion of seeds ≤ 1.57 mm was calculated using statistical analysis as follows:

At 1.20 mm: $p_{1.20\text{mm}} = 0.0099$, $z_{1.20\text{mm}} = -2.33$

At 1.70 mm: $p_{1.70\text{mm}} = 0.2296$, $z_{1.70\text{mm}} = -0.74$

Therefore, 1.57 mm corresponds to a z value of:

$$z_{1.57\text{mm}} = \frac{1.70 - 1.57}{1.70 - 1.20} (-2.33 - (-0.74)) - 0.74 = -1.15$$

This corresponds to a probability of $p_{1.57\text{mm}} = 0.1251$. The verification results are below.

TABLE 8. S2.1 VERIFICATION RESULTS

#	Item	Target Proportion	Measured Proportion	Satisfied (Y/N)
S2.1	Size of smallest grain	0.15	0.1251	Yes

The results predict that less than 12.51% of the grain bulk will fall below the 1.57 mm benchmark, which complies with the initial criteria and S2.1 was considered a pass. However, due to the limitations of the data collection process and assumptions made, it is acknowledged that the client may wish to perform additional verification with the device.

4.2.2. Loading Capacity (S2.2)

S2.2 refers to the design's ability to withstand the grain load in the vertical and lateral directions. S2.2 was verified through calculation in the design stage. The wood plenum must withstand an estimated 5000 kg design load. The maximum estimated load contains a safety factor of 1.5 that accounts for expected variations in bulk density when using organic materials such as grain. The pitot tube supports must also withstand the vertical load of the grain above them. Further, the maximum estimated lateral pressure of the grain must be less than or equal to the allowable load of the perforated metal sheet used in the design.

Design calculations of maximum vertical and lateral pressures, and selected material properties are shown in Appendix C, with the results summarized in the following table. A factor of safety of 2.5 was set for all the structural components.

TABLE 9. S2.2 VERIFICATION RESULTS

#	Item	Maximum Factored Design Load	Failure Load	FOS	Satisfied (Y/N)
S2.2	Lateral pressure on bin wall	484.48 Pa	130 MPa	268	Yes
	Vertical load on plenum	968.97 Pa	8.3 MPa	8.4	Yes
	Vertical load on pitot tube supports	968.97 Pa	248 MPa	255	Yes

All three failure loads are greater than the design loads and S2.2 is satisfied. In the case of the lateral pressure the factor of safety is significantly higher than the desired factor of safety. The high safety factor reflects the minimal amount of lateral pressure exerted by the grain combined with the high strength of steel.

4.3. Instrumentation Specifications (S3.X)

Specifications S3.X define the parameters of the instrumentation implemented in the design and are provided by the respective manufacturers. S3.1 and S3.2 define the pressure reading range and resolution of the two manometers used to read the pitot tubes; S3.3 and S3.4 define the velocity measurement range and resolution of the hot wire anemometer; and S3.5 and S3.6 define the velocity measurement range and resolution of the mass flow sensors. S3.7 defines the fan's output in CFM and revolution speed at approximately 1293 Pa (6 inWG) of static pressure.

Calibration and further verification of the instrumentation implemented in the design is outside the scope of this project and not required for data collection. Parameters provided by the manufacturer can be found in the product specification sheets included in Appendix C. The exception to this is the mass flow sensors which were calibrated for the anticipated airflow range within the system. The calibration procedure is outlined below:

Bench Calibration Procedure for Mass Flow Sensors:

Materials and equipment: mass flow sensors and 3D printed holders; mount to hold sensors; desktop fan with variable velocity; Agilent data acquisition system; hot-wire anemometer; power supply; Benchlink data logger 3 software.

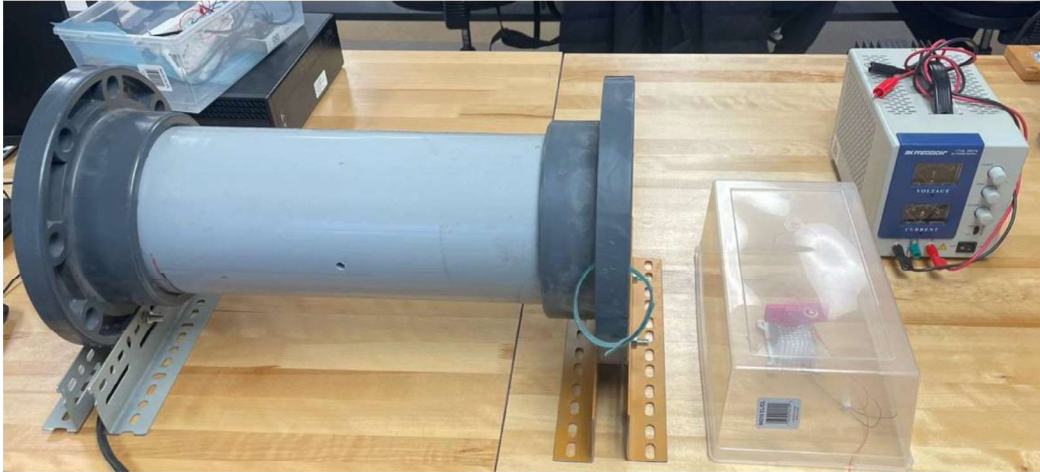


Figure 10. Calibration materials pictured left to right: desktop fan; sensor and 3D printed holder (pink) on calibration mount under plastic box; power supply.

Procedure:

1. The evaluation boards themselves were calibrated first. Then each sensor and its wires were labeled to differentiate between them. Sensors were individually installed into their 3D printed holders.
2. To begin calibration, a sensor was mounted to the calibration setup and connected to the evaluation board. The evaluation board was connected to a data acquisition system and power supply. Data was recorded on the Benchlink data logger 3 software.
3. The sensor was covered with a plastic box to nullify airflow ($V_0=0$ m/s), and the corresponding voltages (U_0) were catalogued and exported with the median voltage value deduced.
4. The fan was then turned on to full power with a velocity of $V_{100} = 6.4$ m/s (checked using the hot-wire anemometer). Then the sensor was placed inside the fan to obtain and record the corresponding voltages and their median (U_{100}).
5. Using the hot-wire anemometer to monitor airflow, the fan's speed was lowered until it reached $V_{50} = 3.2$ m/s. The third voltage values were obtained and their median determined (U_{50}).

- Using the values and equations present in the sensor's manual, a graph was created illustrating the relationship between the airflow speed and the voltage. A separate equation was produced for each sensor to calculate airflow velocity from its voltage reading.

The velocity equations take the form of:

$$\vec{v} = \frac{((U - U_0) * (U + U_0))^{\frac{1}{n}}}{\left(k^{\frac{1}{n}}\right) * U_0^{\frac{2}{n}}}$$

Where U is the measured voltage, n = 0.5, and k is determined by the equation below.

$$k = \frac{\left(\frac{U_{50\%}}{U_0}\right)^2 - 1}{\left(\vec{v}_{50\%}\right)^n}$$

A sample calibration graph is shown below for reference. The full set of calibration graphs and calculated parameters for the mass flow sensors are included in Appendix D.

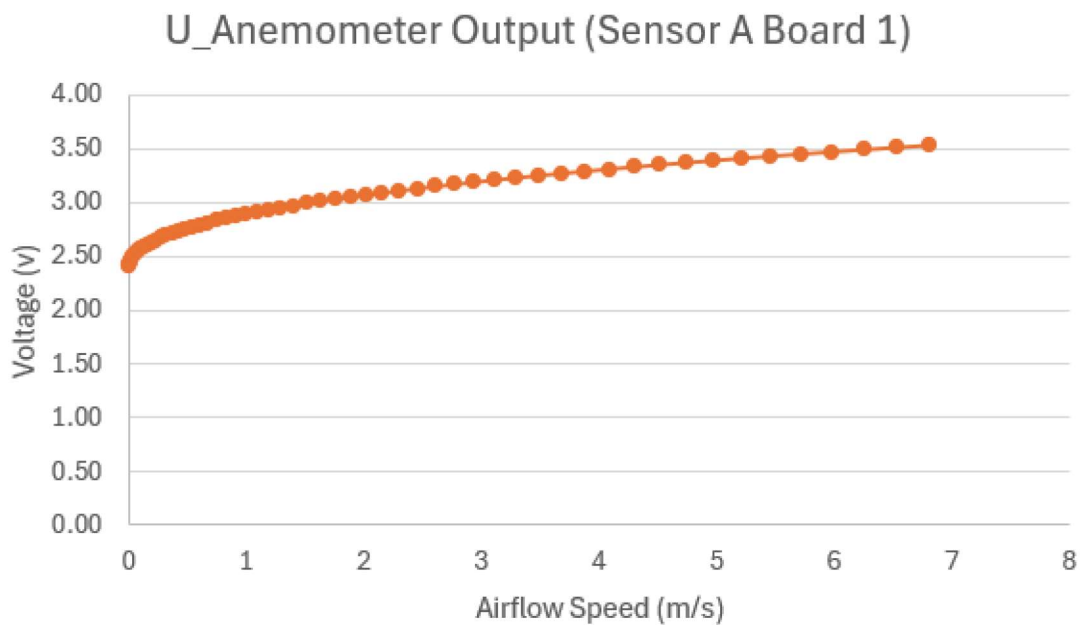


Figure 11. Sample calibration graph for mass flow sensor.

4.4. Airflow Properties (S4.X)

Specifications S4.1 and S4.2 refer to measuring and validating the direction and uniformity airflow through the grain bulk.

4.4.1. Airflow Direction (S4.1)

S4.1 defines the horizontal direction of airflow in the system. S4.1 is considered a pass if the vertical airflow through the top of the grain bulk is measured as zero relative to the air speed of the surrounding ambient air. This confirms that any vertical airflow through the grain is insignificant. The system is designed to create negligible vertical airflow when the bin is filled to the top with grain. All grain was provided by the client, Dr. Fuji Jian, and at the time of testing, not enough wheat was available to fill the bin completely. Therefore, testing was performed with grain filled to a height of 1155 mm.

Airflow was measured using the KANOMAX Anemomaster A031 hot wire anemometer which has a measurement accuracy of $\pm (3\% +0.1)$ m/s. The airflow velocity of the ambient air was measured to be 0.01 m/s and vertical airflow above the bin was measured to be 0.13 m/s.

TABLE 10. S4.1 VERIFICATION RESULTS

#	Item	Target	Measured	Satisfied (Y/N)
S4.1	Vertical airflow	0 m/s	0.13 m/s	No

S4.1 was not satisfied with a grain depth of 1155 mm, and the results are not conclusive. To remediate this for subsequent tests, a plastic tarp was placed on the top of the grain bulk to prevent air from moving upwards and force horizontal airflow. The client was made aware of the issue and expressed that no further verification was required for this specification.

4.4.2. Airflow Distribution (S4.2)

S4.2 defines the radial uniformity of the flow through the bulk. It is verified by measuring the airflow exit velocity from the perforated bin wall of eight evenly distributed points. These points were spaced 45° apart around the circumference of the bin and measured

using a hot wire anemometer. S4.2 is considered a pass if measurements in a radial plane fall within $\pm 10\%$ of the mean. Due to the very low velocity of the air exiting the bin wall, a large cone with a gradual contraction was used to increase the velocity of the airflow to above the threshold of the hot wire anemometer. The inlet and outlet areas of the cone were 0.0674 m^2 and 0.000284 m^2 , respectively. The measured velocity (V_2) and the average exit velocity from the bin (V_1) are related by the equation:

$$V_1 = \frac{A_2}{A_1} * V_2 = \frac{0.000284}{0.0674} * V_2$$

The mean airflow velocity measured was 0.34 m/s and a $\pm 10\%$ variation put the target range at $0.31 - 0.38 \text{ m/s}$. However, two significant outliers were noted in the data with values approximately two times those of the other six readings. Removing these from the mean resulted in an average velocity of 0.27 m/s and a target range of $0.24 - 0.30 \text{ m/s}$. The test results are included in the following table.

TABLE 11. S4.2 VERIFICATION RESULTS

#	Item	Target	Measured	Satisfied (Y/N)
S4.2	Radial Point 1	0.24 - 0.30 m/s	0.27 m/s	Yes
	Radial Point 2	0.24 - 0.30 m/s	0.28 m/s	Yes
	Radial Point 3	0.24 - 0.30 m/s	0.59 m/s	No
	Radial Point 4	0.24 - 0.30 m/s	0.29 m/s	Yes
	Radial Point 5	0.24 - 0.30 m/s	0.24 m/s	Yes
	Radial Point 6	0.24 - 0.30 m/s	0.56 m/s	No
	Radial Point 7	0.24 - 0.30 m/s	0.28 m/s	Yes
	Radial Point 8	0.24 - 0.30 m/s	0.25 m/s	Yes

Six out of eight values fell within the adjusted target range and S4.2 was not completely satisfied. The presence of instrumentation and structural components within the grain bulk are likely the cause of the discrepancies.

4.5. Testing Operations (S5.X)

Specifications S5.X related to how the user interacts with the device during operation. This includes the assembly time, changing the fan and transition, and recording data throughout a test.

4.5.1. Assembly Time (S5.1)

S5.1 is measured by timing how long it takes to assemble the system when input variables are adjusted. The assembly includes attaching the fan and transition system, adjusting the exposed surface area percentage of the internal column, and filling the bin with grain. S5.1 is considered a pass if the assembly time takes less than four hours when the bin starts from empty.

The total assembly time was measured during the testing and verification phase of the design. Steps 1 and 2 of the data collection procedure in Table 3 (system assembly and grain loading) were timed with the results recorded below.

TABLE 12. S5.1 VERIFICATION RESULTS

#	Item	Target	Measured	Satisfied (Y/N)
S5.1	System assembly time		1.5 hours	
	Grain loading time		2.25 hours	
	Total time elapsed	<4 hours	3.75 hours	Yes

4.5.2. Adjustability for Fans and Transitions (S5.2)

S5.2 is defined by the system's compatibility with varying transitions. This specification is verified by measuring that the fan securely connects to the transition and the transition connects securely to the plenum without air leakage. S4.5 will be considered a pass for all transitions if there is a zero reading by the hot wire anemometer relative to the ambient air at the transition's connection points. Similarly to S4.1, the values were read by the KANOMAX A031 hot wire anemometer and were rounded to one decimal place.

TABLE 13. S5.2 VERIFICATION RESULTS

#	Item	Target	Measured	Satisfied (Y/N)
S5.2		0 m/s	0.01 m/s	Yes

The difference between the two measurements rounded to zero and S5.2 was satisfied.

4.5.3. Measurement Frequency and Test Length (S5.3, S5.4)

Specifications S5.3 and S5.4 refer to the frequency of pressure and velocity readings taken from the device during testing. Manual measurement readings and test duration times were verified through observation of a stopwatch during testing. Further verification or automation of measurement times are not required for the scope of this project.

5. SUSTAINABILITY

To ensure the project's success in other areas other than engineering and design, Team 8 conducted a sustainability evaluation of its long-term impact on the community and the environment. The project was evaluated using Green Project Management (GPM) P5 Impact Analysis Version 5.0.2 [10] and Triple Bottom Line (TBL) framework [11] which were adopted by The University of Waterloo's Engineering Faculty in assessing projects.

Triple Bottom Line recognizes the connection between the planet, people and prosperity in relation to the project. Green Project Management defines elements, proposed actions, potential impact for the proposed action scored from 1 (severe negative impact) to 5 (strong positive impact). Each of the five selected sustainability elements in Table 14 is evaluated using an impact score, showing the overall change in impact before and after proposed or implemented sustainability measures.

TABLE 14. GPM SUSTAINABILITY ANALYSIS

Planet Impact 1: Category – Transport (Scored: YES)		
Element	Local Procurement	
Description	Local procurement is the practice of purchasing products and services from local suppliers.	
Description Cause	Materials used in assembling and testing the prototype are purchased from local suppliers such as Home Depot, Metal Supermarket, and All Size Perforating Ltd.	
Potential Sustainability	Incorporating locally purchased materials into the project contributes to the economic vitality, reduced carbon footprint as materials are transported over short distances leading to lower fuel consumption and emissions.	
Proposed Response	Future modification made to the project and grains used in testing should be purchased from local suppliers throughout the life span of the project.	
Impact Scores		Before: 4
		After: 5
		Change: 1

TABLE 14. GPM SUSTAINABILITY ANALYSIS - CONTINUED

Planet Impact 2: Category – Energy (Scored: YES)		
Element	Energy Consumption	
Description	Energy consumption is the amount of energy used by the project throughout its duration. It encompasses all aspects of energy use from office lighting to the energy required for transportation.	
Description Cause	Existing grain silos typically require high amount of energy to effectively dry grains.	
Potential Sustainability	The iterated prototype is projected to yield energy savings through reduced power consumption and enhanced grain drying efficiency.	
Proposed Response	Future design operating systems modification made to the project should prioritize reduced power consumption as the key element of the sustainability strategy	
Impact Scores		Before:3
		After: 4
		Change: 1
People Impact 1: Category – Society and Customers (Scored: YES)		
Element	Customer Health and Safety	
Description	Customer health and safety includes the measures taken to ensure the physical and mental wellbeing of the end users of the project's results. This includes providing information about risks and hazards, proper customer handling during the project, and adherence to relevant safety standards, protocols, laws, and regulations.	
Description Cause	The prototype does not provide any information regarding potential risks or hazards that come with assembling and using the grain storage bin.	
Potential Sustainability	Students collecting data might face pinch hazards, ergonomic hazards that come with loading and unloading 3000kg of grains.	
Proposed Response	A manual should be prepared indicating potential hazards, personal protective equipment's required when loading grains, unloading grains, and during operation.	
Impact Scores		Before:1
		After: 4
		Change: 3

TABLE 14. GPM SUSTAINABILITY ANALYSIS - CONTINUED

People Impact 2: Category - Labor Practices and Decent Work (Scored: YES)		
Element	Training and Qualifications	
Description	Training and qualifications are the process of ensuring that operators have the necessary skills to effectively complete their work. It involves providing instruction, assessing proficiency, monitoring performance, and offering guidance.	
Description Cause	The grain storage bin uses calibrated mass flow sensors that are sensitive, easy to break and require careful handling, hot wire anemometer and digital manometer in reading data and a data acquisition system.	
Potential Sustainability	Training on sensor calibration, placement, and data acquisition system connection was provided to team members and the client's Ph.D. student for effective data collection.	
Proposed Response	Future students using the grain storage bin in conducting research should consult with the University of Manitoba Biosystems Engineering technicians for training on calibration, replacement of the mass flow sensors, usage of hot wire anemometers, digital anemometer and data acquisition system before conducting their research.	
Impact Scores		Before:3
		After: 4
		Change: 1
Prosperity Impact: Category – Local Economic Impact (Scored: YES)		
Element	Indirect Benefits	
Description	Indirect benefits are the positive impacts that go beyond the immediate outcomes of the project and may not always be immediately visible. These benefits can include improved quality of life, increased economic activity in the local area, and environmental improvements such as cleaner air or water.	
Description Cause	The grain storage bin is used to conduct research and collect more data on horizontal aeration of different grains.	

TABLE 14. GPM SUSTAINABILITY ANALYSIS - CONTINUED

Potential Sustainability	Data collected is used to show the effectiveness of horizontal grain aeration compared to vertical grain aeration.	
Proposed Response	The data collected and research findings are to be shared with local farmers to enhance both moisture control and grain quality within grain storage bins.	
Impact Scores		Before: 3
		After: 4
		Change: 1

The overall lifespan lens project score under Green Project Management indicates an initial average score evaluation of 2.8 on the existing project, a news average score of 4.2 upon implementation of proposed responses. The overall change is 1.4, indicating neutral impact throughout the lifespan of the project.

6. CONCLUSION

This project developed a functioning horizontal grain aeration testing and measurement system for use in Ph.D. research at the University of Manitoba. The system was designed to provide data to support the development of, and verify, computational models of different horizontal grain aeration systems. The models will predict the effects that changing ventilation components have on airflow. The system functions by forcing air horizontally through the system, where pressure and velocity are measured at several key locations in its travel path. Five measurement layers ensure that sufficient data is recorded. The design is adjustable to allow for future testing with different grain types and ventilation configurations.

Testing and verification of the device was conducted using wheat, and the results demonstrated that the system operates as intended. It is compatible with seed sizes greater than 1.57 mm and can withstand the vertical and lateral pressures imposed by the grain bulk. It is assumed that when full it allows for negligible airflow in the vertical direction, though this could not be verified at the time of testing. Airflow was primarily uniform radially, but some variability was observed and attributed to the effect of instrumentation within the device.

These results show that the system provides meaningful data for future studies. Client feedback confirmed that the results met the project expectations, proving the design's effectiveness. With continued testing and refinement, this device will contribute to a better understanding of horizontal grain aeration systems and help improve grain storage practices.

6.1. Project Limitations

A major limitation in the design is the necessary presence of instrumentation to retrieve the required data for analysis. Any instrumentation naturally disrupts the airflow path and can affect the accuracy of the desired measurement. The presence of the mass flow sensors in the internal column may also disrupt the radial uniformity of the airflow exiting the column and introduce additional turbulence. For the design stage to proceed, this error had to be assumed negligible enough to collect acceptable data. While this problem is impossible to avoid completely, the design attempted to mitigate these effects by providing adequate space between the pitot tube sets and minimizing the size of their support structure as much as possible. The

support structure and 3D printed mounts for the mass flow sensors were designed to be thin and minimally intrusive. However, non-uniformity was still observed in the airflow exiting the bin wall and thought to be attributed to the presence of the physical objects within the device.

The individual resolutions and accuracies of the instrumentation implemented in the design limit the precision of the data that can be collected from the system. Each device has its own associated error and tolerances which compound to produce an error for the overall design. Devices may react differently to varying external conditions, such as temperature and relative humidity levels of the air. This means that any results collected from the device should be considered in conjunction with the air properties at that time. It is also important to consider that air properties will differ depending on where in the system the data is collected, as the air in the internal column will respond to the temperature and moisture levels of the grain it interacts with. The device was constructed and verified in an indoor environment which was assumed to be relatively stable. However, no additional measures were taken to maintain a controlled environment within the room. Any effect on the instrumentation from fluctuating environmental conditions was assumed to be negligible.

Due to the inability to acquire the volume of grain to fill the entire bin, verification tests had to be completed using a plastic tarp to prevent airflow from travelling vertically through the system. This presented a challenge in verifying the technical specifications related to airflow travel path and uniformity. Tests were completed as outlined in the verification procedure section, however, the specification defining completely horizontal airflow could not be verified at the time of testing.

Further limitations in the test methodology and results arose from the sieve analysis performed to assess the device's compatibility with the canola seed available in the on-campus lab. The sieve aperture sizes were only available in 1.70 mm and 1.18 mm dimensions which did not coincide with the 1.57 mm perforation size of the bin wall that defined the specification. Therefore, the test methodology had to approximate the percentage of canola falling below the perforation diameter using statistical distribution. This should be held in consideration when evaluating the results of the test and subsequent passing of the criteria.

Calibrating sensors in the system in which they are to be used is preferred for accuracy and validity of results. Given the impracticality of and challenges associated with calibrating the

sensors while enclosed by the internal column, a bench top calibration was performed on all ten sensors. While they were calibrated for the expected range of velocities they encounter within the device, the environmental conditions the sensors experience during testing cannot be perfectly replicated in the lab. In the lab setting, airflow was directed perpendicularly across the sensor surface in a relatively controlled path. In reality, there is likely turbulent airflow within the column that creates significantly different airflow patterns. The effect of cross-directional airflow is unknown and may interfere with the accuracy of the velocity measurements obtained.

6.2. Recommendations

It is recommended that future prototypes of similar testing and measurement systems consider less intrusive measurement options to reduce the interference of instrumentation on the airflow. This includes the pitot tubes, pitot tube support structure, and the mass flow sensor setup. Minimizing any structures within the grain bulk will also ensure that the bulk remains uniform throughout the bin. To further improve the data collection methods, it is suggested that the number of manual measurements required be reduced by incorporating automated data collection systems where possible. Future calibration of the mass flow sensors should be performed within the device to maximize the reliability of their readings. Incorporating these recommendations into the design will improve the accuracy of the data and the efficiency with which it is collected. Additionally, a smaller perforation size for the exterior bin would expand the range of seed diameters compatible with the device, thus increasing the device's functionality and applications.

The next step is to use the constructed device to inform the modelling of horizontal airflow systems. This involves following the outlined operation procedure to collect data across different system configurations. The resulting model will help analyze how pressure drops vary in response to changes in the system design. Other design options may be considered at this point as the scope of this project was limited to aerating grain only to the height of the inlet. As research progresses to full-scale testing, designs that address aeration of the entire grain depth are recommended for modelling and optimization.

Encouraging more research in this area will provide manufacturers with the necessary data to develop functional horizontal aeration systems for full-scale grain bins. Additionally, farmers would feel more confident in adopting systems developed with measurable data, particularly if the benefits compared to vertical aeration are quantifiable. This project is a step towards reducing the time and energy demands of grain aeration that farmers currently operate under, promoting continual growth and innovation within the industry.

REFERENCES

- [1] F. Jian and D.S. Jayas, *Grains: engineering fundamentals of drying and storage*. Boca Raton: CRC Press, 2021.
- [2] C. Jones and J. Hardin, "Aeration and Cooling of Stored Grain," *okstate.edu*, Feb. 2017. [Online]. Available: <https://extension.okstate.edu/fact-sheets/print-publications/bae/aeration-and-cooling-of-stored-grain-bae-1101.pdf><https://extension.okstate.edu/fact-sheets/aeration-and-cooling-of-stored-grain.html>. [Accessed Sept. 30, 2024].
- [3] S. Navarro and R. Noyes, *The mechanics and physics of modern grain aeration management*. Boca Raton: CRC Press, 2002.
- [4] S. Neethirajan, C. Karunakaran, D.S. Jayas, and N.D.G. White, "X-ray Computed Tomography Image Analysis to explain the Airflow Resistance Differences in Grain Bulks," *Biosystems Engineering*, vol. 94, no. 4, pp. 545-555, 2006. [Online]. Available: <https://www.sciencedirect.com.uml.idm.oclc.org/science/article/pii/S1537511006001504>. [Accessed Oct. 1, 2024].
- [5] N.R. Boopathy, "Segregation of canola, kidney bean and soybean in wheat during bin loading," M.S. thesis, University of Manitoba, Winnipeg, MB, 2018. [Online]. Available: <https://mspace.lib.umanitoba.ca/items/a85f6676-35ab-4f27-a856-7710c619eb14>. [Accessed Oct. 1, 2024].
- [6] V. Chelladurai, V.R. Parker, D.S. Jayas, and N.D.G. White, "Evaluation of a Horizontal Air Flow In-Bin Grain Drying System," *Applied Engineering in Agriculture*, vol. 31, no. 5, pp. 793-797, 2015. [Online]. Available: <https://elibrary-asabe.org.uml.idm.oclc.org/abstract.asp?aid=46400&t=3&dabs=Y&redir=&redirType=>. [Accessed Oct 1, 2024].
- [7] C. Nwaizu and Q. Zhang, "Computational modeling of heterogenous pore structure and airflow distribution in grain aeration system," *Computers and Electronics in Agriculture*, vol. 188, 2021. [Online]. Available: <https://www.sciencedirect.com.uml.idm.oclc.org/science/article/pii/S016816992100332X>. [Accessed Oct. 1, 2024]

- [8] A. Sadeghizadeh, "Characterization of Airflow Resistance of Different Moisture Content Wheat Bulks Mixed with Different Percentages and Sizes of Dockage," M.S. thesis, University of Manitoba, Winnipeg, MB, 2023. [Online]. Available: <https://mspace.lib.umanitoba.ca/items/6ed5542f-fb66-4383-b950-5e89c474faca>. [Accessed Oct. 1, 2024].
- [9] ASABE, "ANSI/ASAE S319.5 AUG2023: Method of determining and expressing fineness of feed materials by sieving," *American Society of Agricultural and Biological Engineers*, Aug. 2023.
- [10] Green Project Management (GPM), "P5 Impact Analysis Version 5.0.2,," [Online]. Available <https://greenprojectmanagement.org/gpm-standards/the-p5-standard-for-sustainability-in-project-management>. . [Accessed Dec. 4, 2024].
- [11] J. Elkington, "Triple Bottom Line," [Online]. Available: <https://johnelkington.com/archive/TBL-elkington-chapter.pdf>. [Accessed Dec. 2, 2024].
- [12] J. Horabik and M. Molenda, "Properties of Grain for Silo Strength Calculation," in *Physical Methods in Agriculture*, J. Blahovec and M. Kutílek, Eds. Boston, MA: Springer, 2002, pp. 137–172. doi: 10.1007/978-1-4615-0085-8_12.
- [13] IST AG, "FS7.0.1L.195 Thermal Mass Flow Sensor" *IST AG*, [Online]. Available: <https://www.ist-ag.com/en/products/thermal-gas-flow-sensor-fs7>. [Accessed: Mar. 20, 2025].
- [14] Dwyer Instruments, "160 Series Pitot Tubes," *ITM Instruments*, [Online]. Available: <https://www.itm.com/pdfs/cache/www.itm.com/160-series/datasheet/160-series-datasheet.pdf>. [Accessed: Mar. 20, 2025].
- [15] Kanomax, "A031 Operation Manual," *Kanomax USA*, [Online]. Available: https://kanomax-usa.com/wp-content/uploads/2021/03/A031_Manual.pdf?x16379. [Accessed: Mar. 20, 2025].
- [16] REED Instruments, "R3030/R3100 Digital Manometer Instruction Manual," *REED Instruments*, [Online]. Available: <https://www.reedinstruments.com/pdfs/cache/www.reedinstruments.com/r3030/manual/r3030-manual.pdf>. [Accessed: Mar. 20, 2025].

APPENDIX A: BILL OF MATERIALS

The table below shows the cost of different parts of the design that were provided by Dr. Jian and the tools purchased to aid the completion of our project. The price of parts provided by the client is unknown, hence indicated with N/A in the cost section. All other parts and materials were bought by the team with a combination of funding provided by Dr. Mann and AAFC. The materials are grouped in order of their respective subsystems, then by the subassembly, and finally by the individual components.

TABLE A1. BILL OF MATERIALS

Item	Brand/Manufacturer & Part Number/Model	Supplier	Quantity	Unit Cost	Total Cost (before tax)
Components for the Plenum Subsystem					
Subassembly: Octagonal plenum					
Plywood sheets	4-foot x 8-foot x 7/16-inch Oriented Strand Board Model # 108771	Home Depot	5	\$21.22	\$106.1
2x4 Lumber	2-inch x 4-inch x 10-ft SPF Select 2Btr Grade Lumber	Home Depot	11	\$7.95	\$87.45
Adhesive	LePage No More Nails Wet Grab Construction Adhesive, White, Interior/Exterior, Waterproof, 266 ml Model # 2073546	Home Depot	2	\$16.54	\$33.08
Subassembly: Ventilation					
Northern Blower	CML NORTHERN BLOWER INC. Size: 6, DES.: 7993 Serial # A42635-2	Dr. Jian	1	N/A	N/A

Transition	N/A	Dr. Jian	1	N/A	N/A
Ball valve	N/A	Dr. Jian	1	N/A	N/A
Components for the Bin Subsystem					
Subassembly: External Column and Supports					
2' x 10' perforated metal sheets	PM-Steel-1008-Round Hole, 20 (0.036") – 063/093 – 4'x10' Perforated Metal (cut into 2'x10' + freight)	All Size Perforating Ltd.	10	N/A	\$1506.75
0.5" x 0.125" 3 ft. steel bars	30" of Hot Rolled Flat Bar 0.125" X 0.500" HF/125500	Metal Supermarket	16	\$2.7612	\$44.18
Subassembly: Internal Column					
Perforated column and lid	N/A	Dr. Jian	1	N/A	N/A
Plastic sheeting	HDG 12 ft. x 14 ft. Light Duty Tarp in Blue (2-Pack) Model # KS2LDCB1214	Home Depot	1	\$22.37	\$22.37
Subassembly: Door					
Sheet metal for discharge chute, and door frame	Zinc-Galvanized Low-Carbon Steel Sheet, 24" x 48" x 0.036" 8943K16	McMaster-Carr	1	\$53.24	\$53.24
Components for the Measurement Subsystem					
Subassembly: Pressure Measurement					
Pitot Tube	Dwyer Series 160-36 Stainless Steel Pitot Tube (5/16" dia. X 36"L)	ITM Instruments Inc.	5	\$270	\$2614.42

Pitot Tube	Dwyer Series 160-24 Stainless Steel Pitot Tube (5/16" dia. X 24"L)	ITM Instruments Inc.	5	\$238	
Pitot Tube Support Frame	Hot Rolled Square Bars (0.375" X 20") HSQ/375	Metal Supermarket	14	\$3.6782	\$ 51.49
Pitot Tube Support Frame	Hot Rolled Square Bars (0.375" X 24") HSQ/375	Metal Supermarket	4	\$4.41384	\$ 17.66
Digital Manometer	REED Model: R3030/R3100	Dr. Jian, Minami Maeda	2	N/A	N/A
Hot-wire Anemometer	KANOMAX Anemomaster A031	Dr. Jian	1	N/A	N/A
Thermal Mass Flow Sensors	Innovative Sensor Technology FS7.0.1L.195	Digi-key	15	\$17.39	\$260.85
Mass Flow Sensor Boards	Innovative Sensor Technology FS FLOWMODULE	Digi-key	2	\$312.33	\$624.66
Electric Box	Carlson 6 x 6 x 6 D. 216 cu in. Weatherproof Junction Box with Cover # E989RRR-V2-UPC	Home Depot	1	\$ 39.98	\$ 39.98
Electric Box Cord Grip	Carlson Nylon cord grip grey fitting 3/4 in. # CGC-075-V2	Home Depot	1	\$ 10.98	\$10.98
Electric Box Cord Grip	Carlson Nylon cord grip grey fitting 3/8 in. # CGC-038-V2	Home Depot	1	\$ 6.28	\$6.28

Power Supply	BK Precision 1730A DC Power Supply	Daniel Benedet	1	NA	N/A
Data Acquisition Unit	Agilent(/Keysight) Data Acquisition System/Data Logger 34972A	Daniel Benedet	1	N/A	N/A
2-Pole Rotary Switch	MFG: E-Switch / KC25A9.501NLS Part # EG5866-ND	Digi-key	2	\$10.91	\$21.82
Knob Fluted W/Skirt 0.250" Phen	MFG: Davies Molding, LLC / 1105 Part # 1722-1048-ND	Digi-key	2	\$2.46	\$4.92
Subassembly: Uniformity Measurement					
Testing and Miscellaneous Materials					
Wheat	N/A	Dr. Jian	1	N/A	N/A
Metal mesh for bin door	N/A	Dale Bourns	1	N/A	\$70
Wire Extensions and Electrical Connections	N/A	Daniel Benedet, Minami Maeda	1	N/A	
Hardware	Bolts, nuts, washers, rivets, etc.	Dale Bourns, Daniel Benedet, Minami Maeda	1	N/A	
Screws	Paulin #8 x 1-inch Flat Head Square Drive Construction Screws in Yellow Zinc – 100pcs Model # 214-630	Home Depot	1	\$7.17	

Screws	Paulin #8 x 2-inch Flat Head Square Drive Construction Screws in Yellow Zinc – 100pcs Model # 214-633	Home Depot	1	\$11.98	\$11.98
Cutting Services	N/A	Metal Supermarket	1	\$18.0	\$18.0
Total Cost					\$5613.38

APPENDIX B: ENGINEERING DRAWINGS

Appendix B contains detailed engineering drawings of different parts contained in the design of the Horizontal Grain Aeration Testing and Measurement System. This includes drawings for the:

- Pitot tube support structure
- Plenum
- Side door
- 3D printed sensor mounts

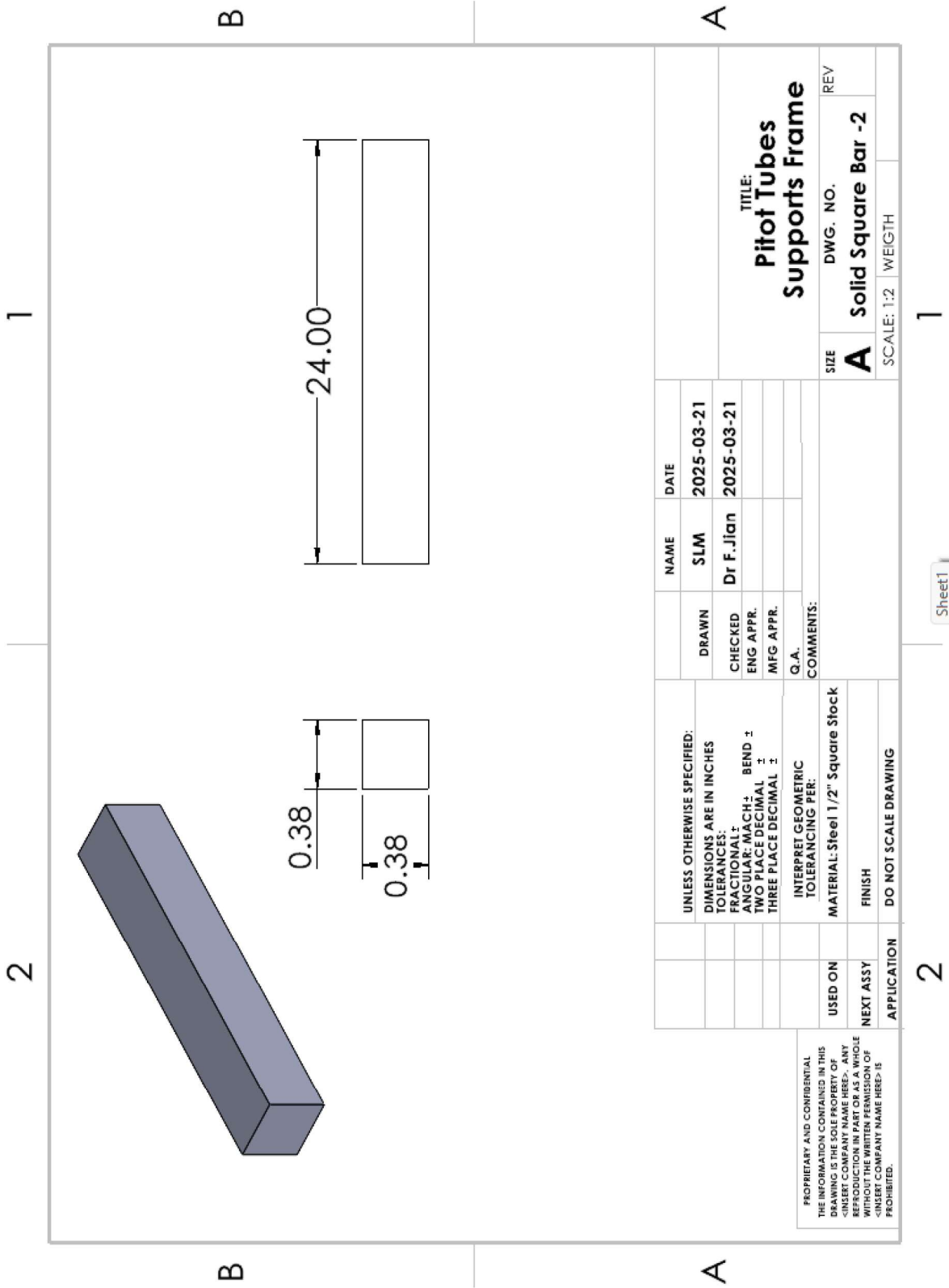


Figure B2. Detailed engineering drawing of the solid square bar-2.

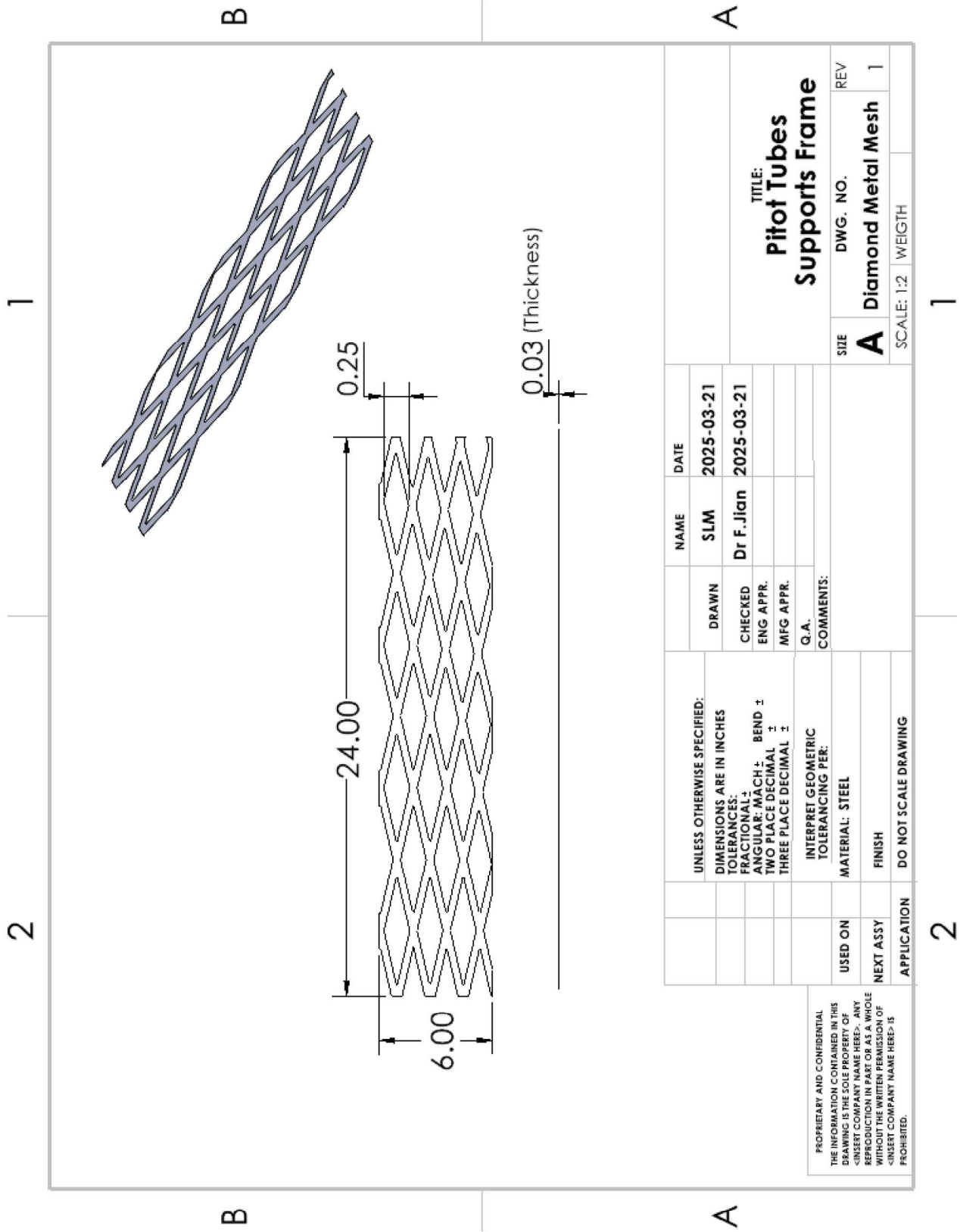


Figure B3. Detailed engineering drawing of the diamond metal mesh.

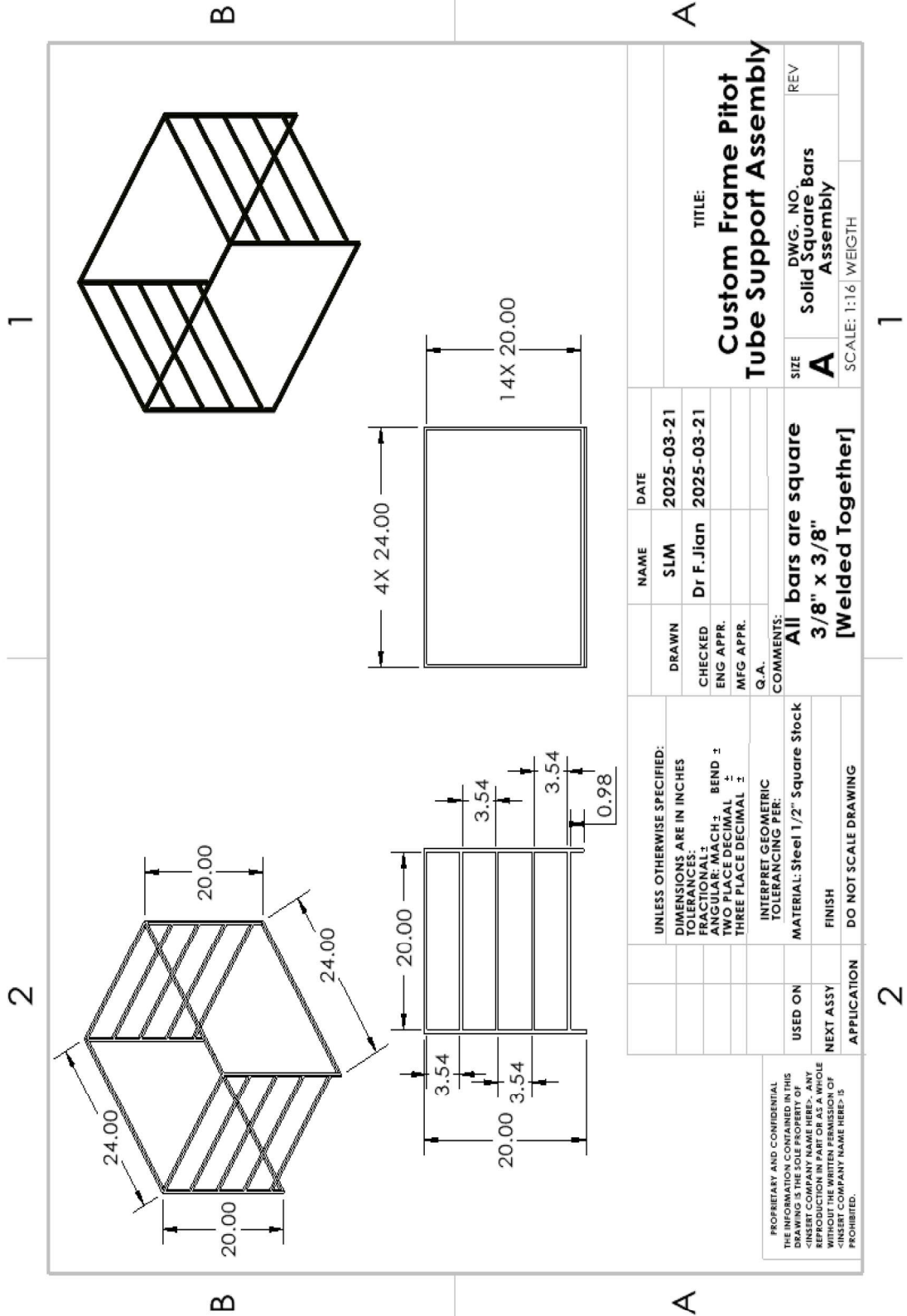


Figure B4. Detailed engineering drawing of the square bar assembly.

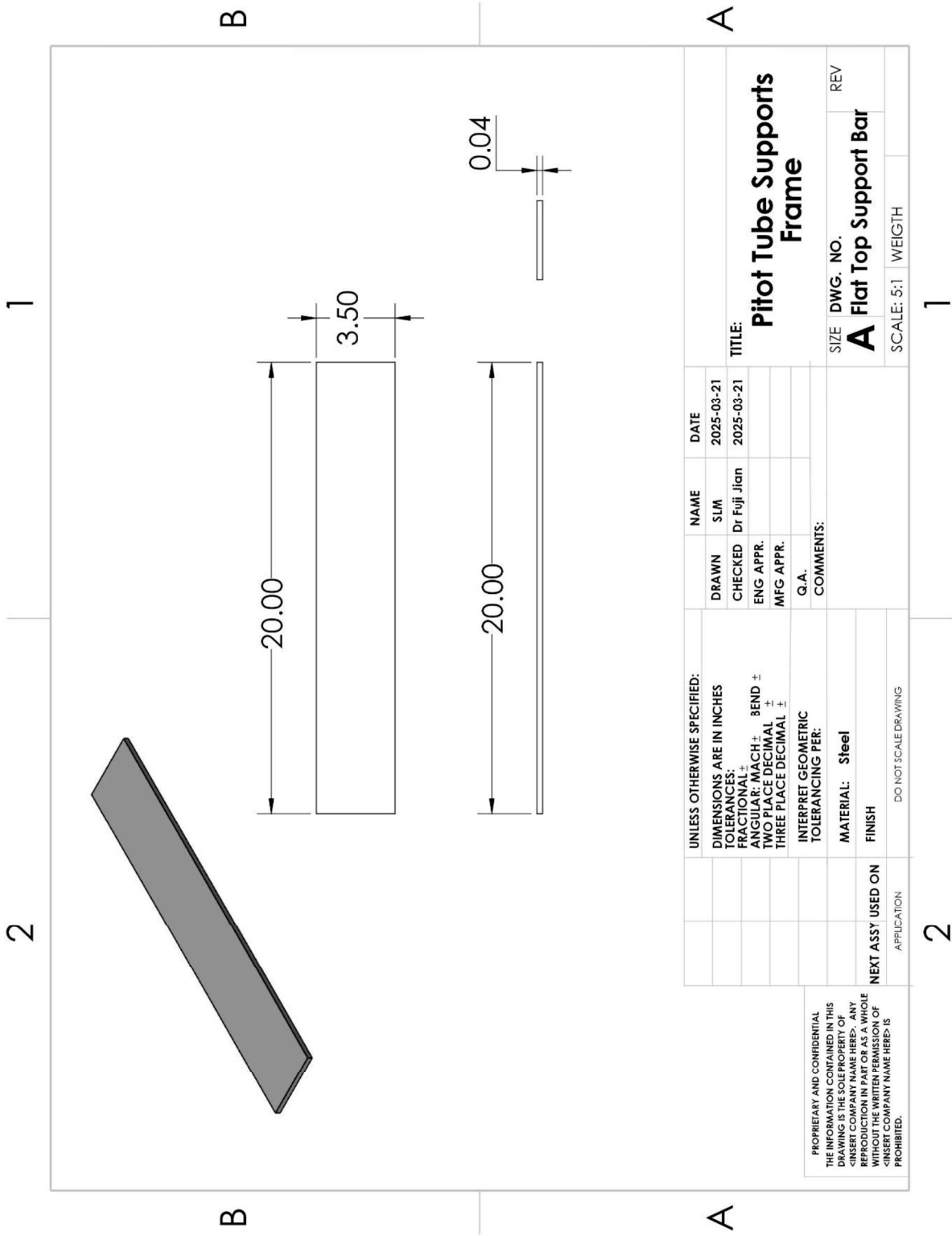


Figure B5. Detailed engineering drawing of the flat top support bar.

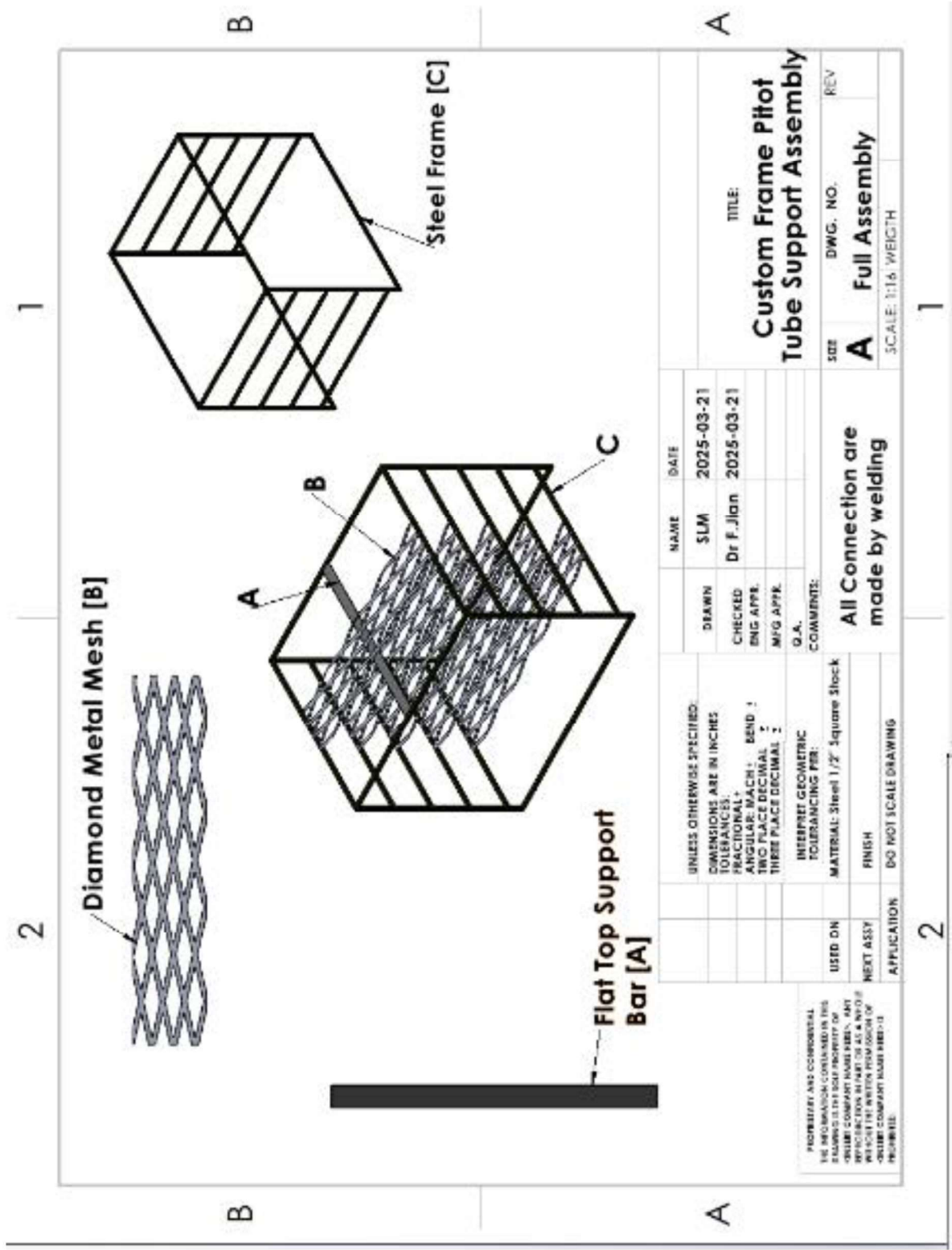


Figure B6. Detailed engineering drawing of the full subsystem assembly showing placement of the diamond metal mesh, flat top support bar.

Plenum

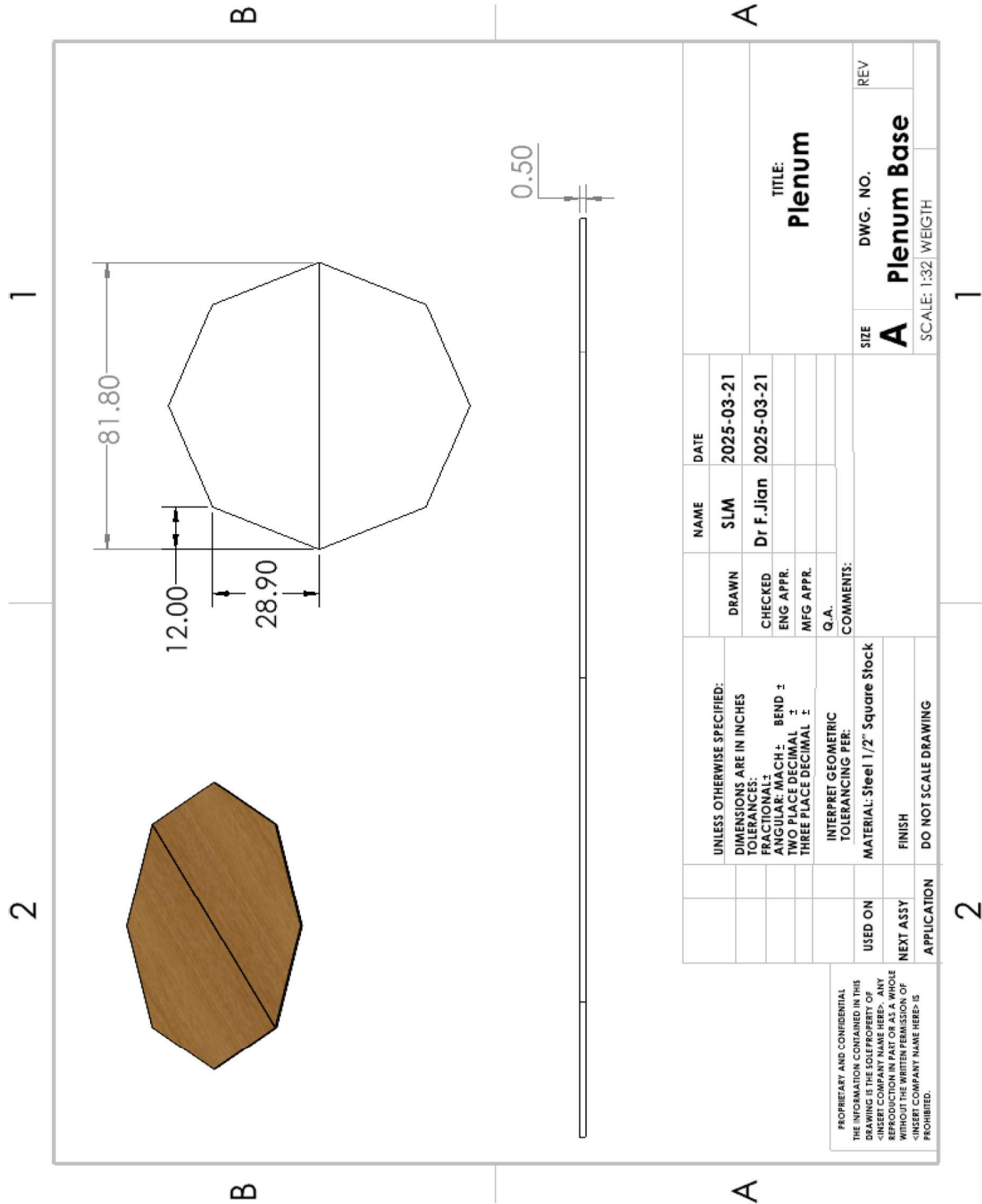


Figure B7. Detailed engineering drawing of the plenum base.

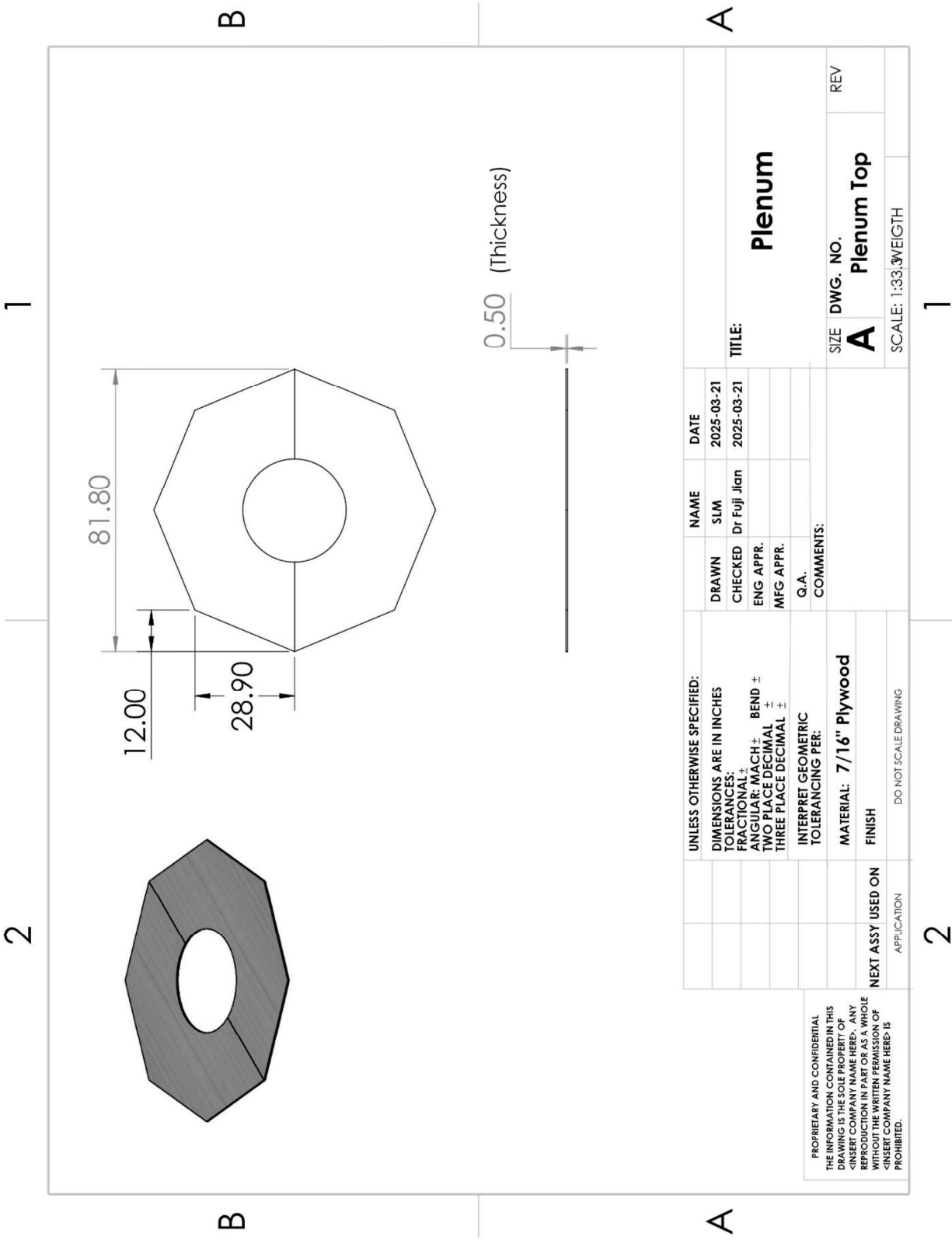


Figure B8. Detailed engineering drawing of the plenum top.

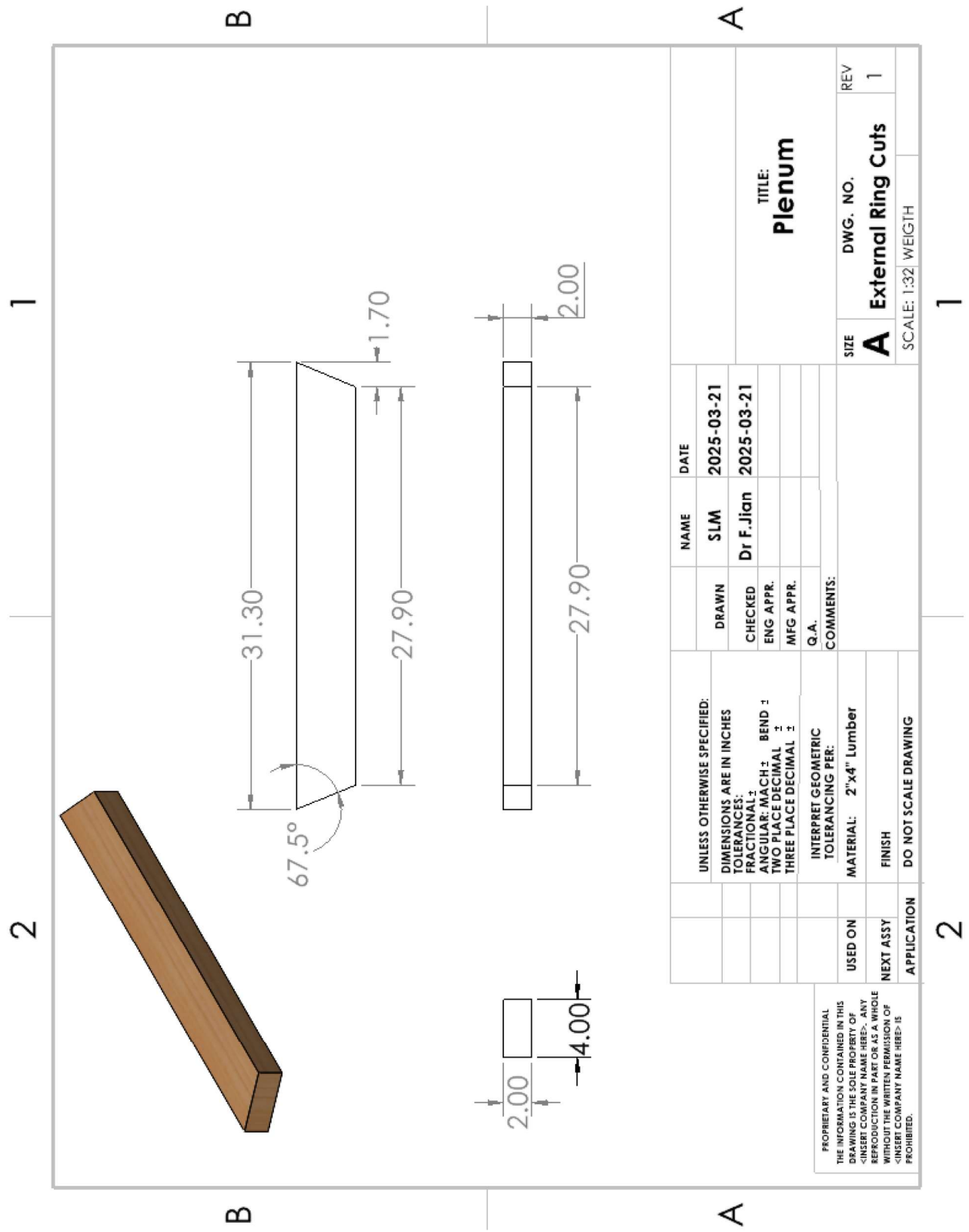
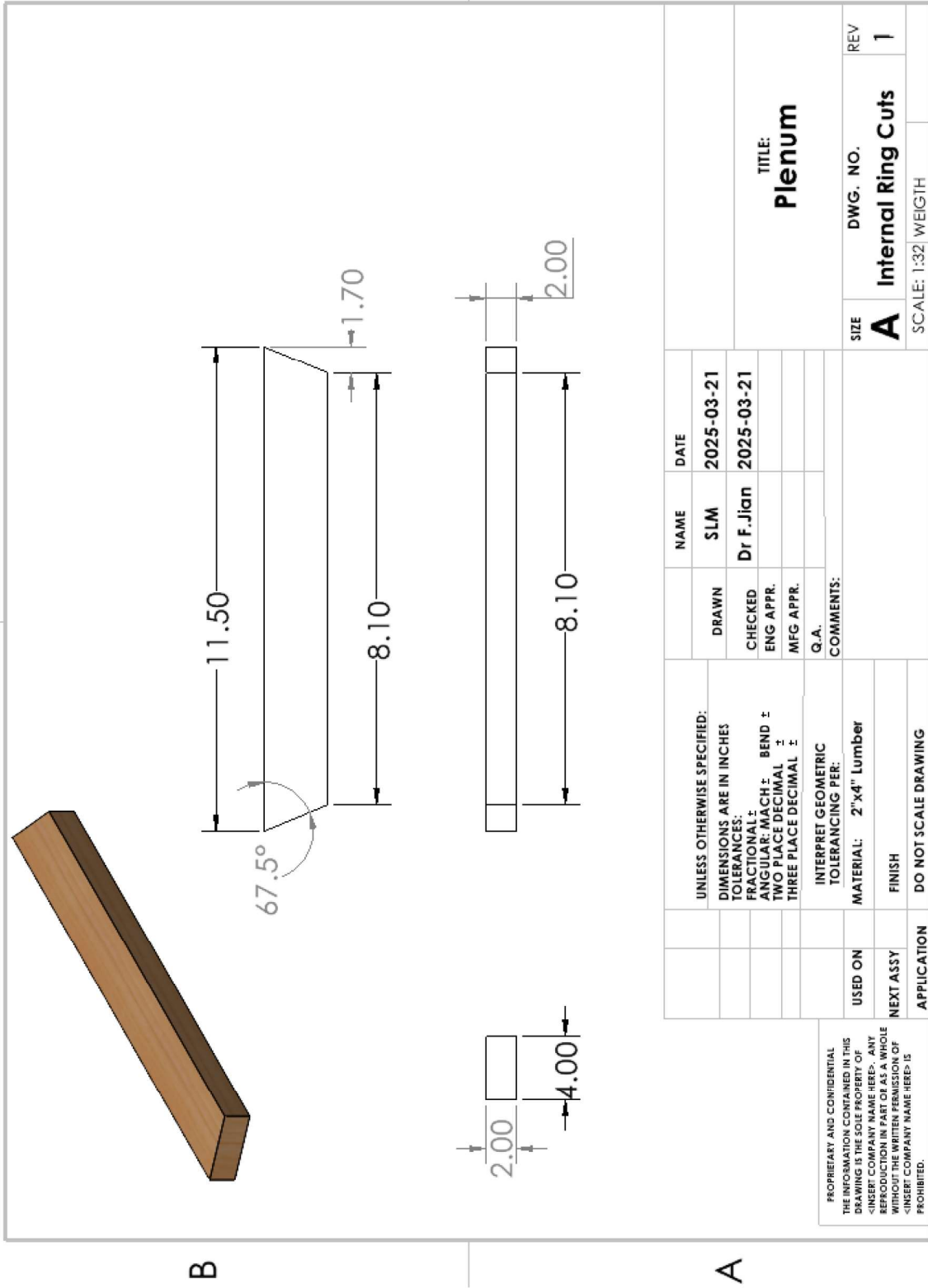


Figure B9. Detailed engineering drawing of the external ring cuts.

2 1



2 1

Figure B10. Detailed engineering drawing of Internal ring cuts.

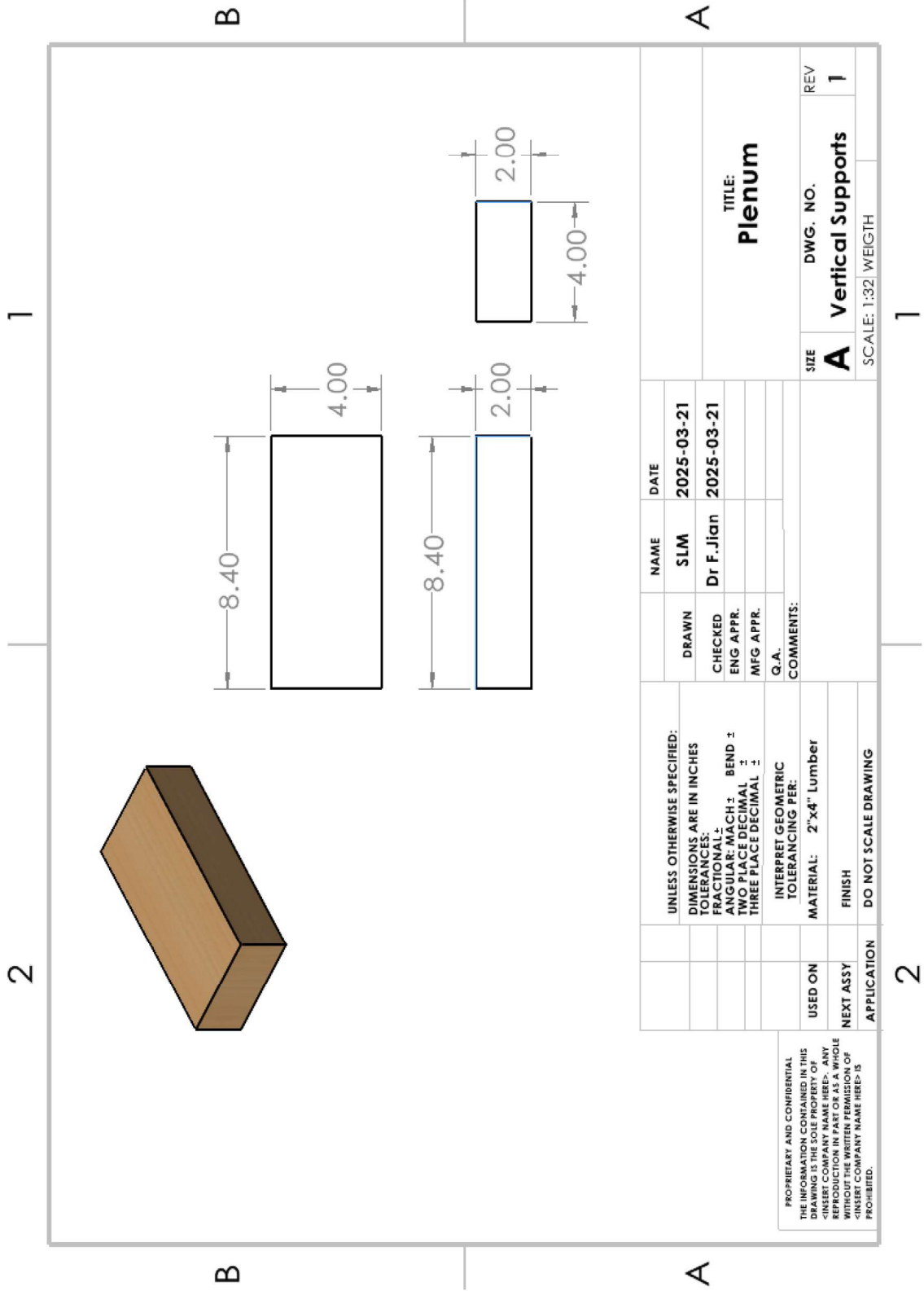


Figure B11. Detailed engineering drawing of the vertical supports.

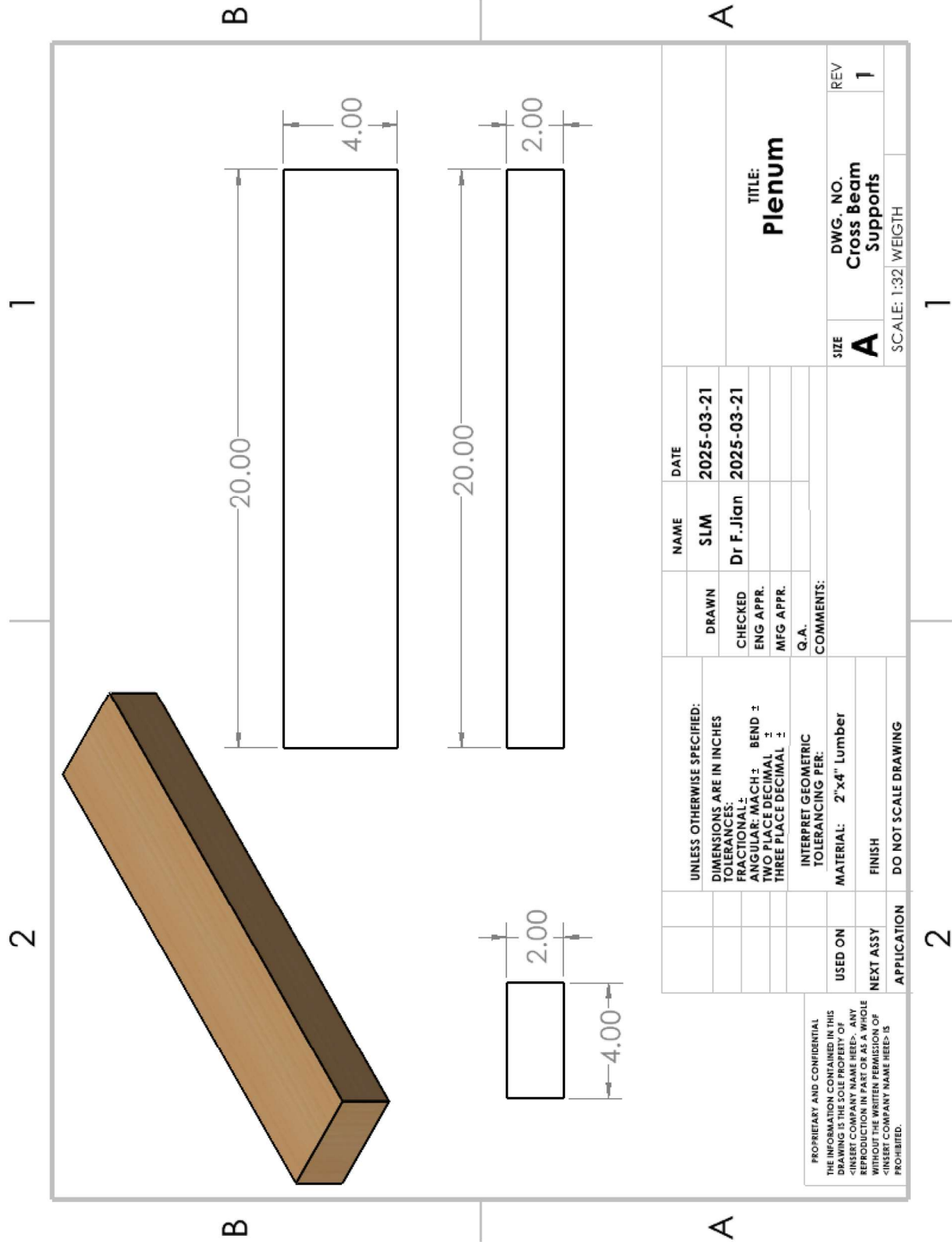


Figure B12. Detailed Engineering drawing of the Cross Beam Supports.

Side Door

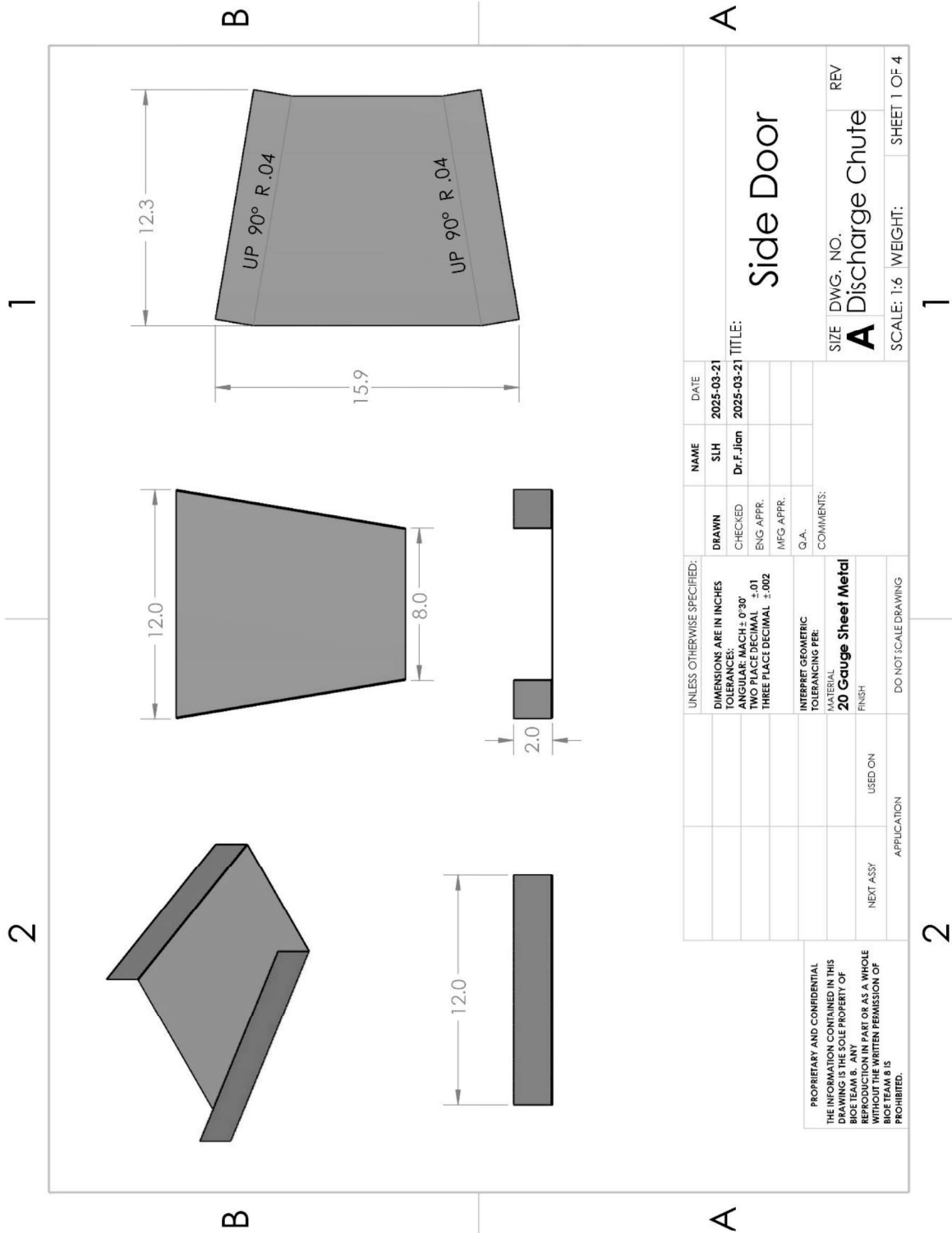


Figure B14. Detailed engineering drawings of the discharge chute on the side door.

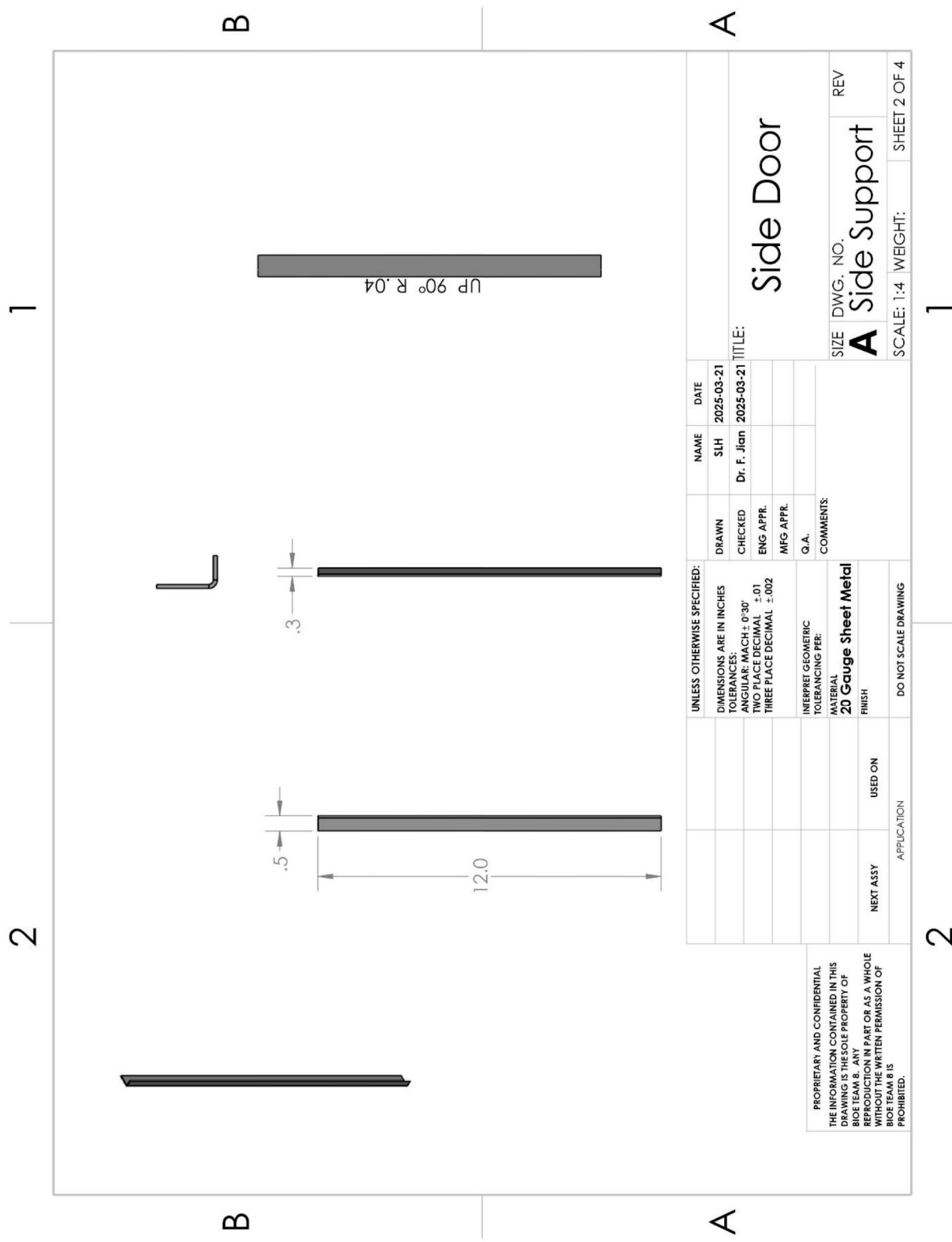


Figure B15. Detailed engineering drawings of the side support on the side door.

3D Printed Sensor Mounts

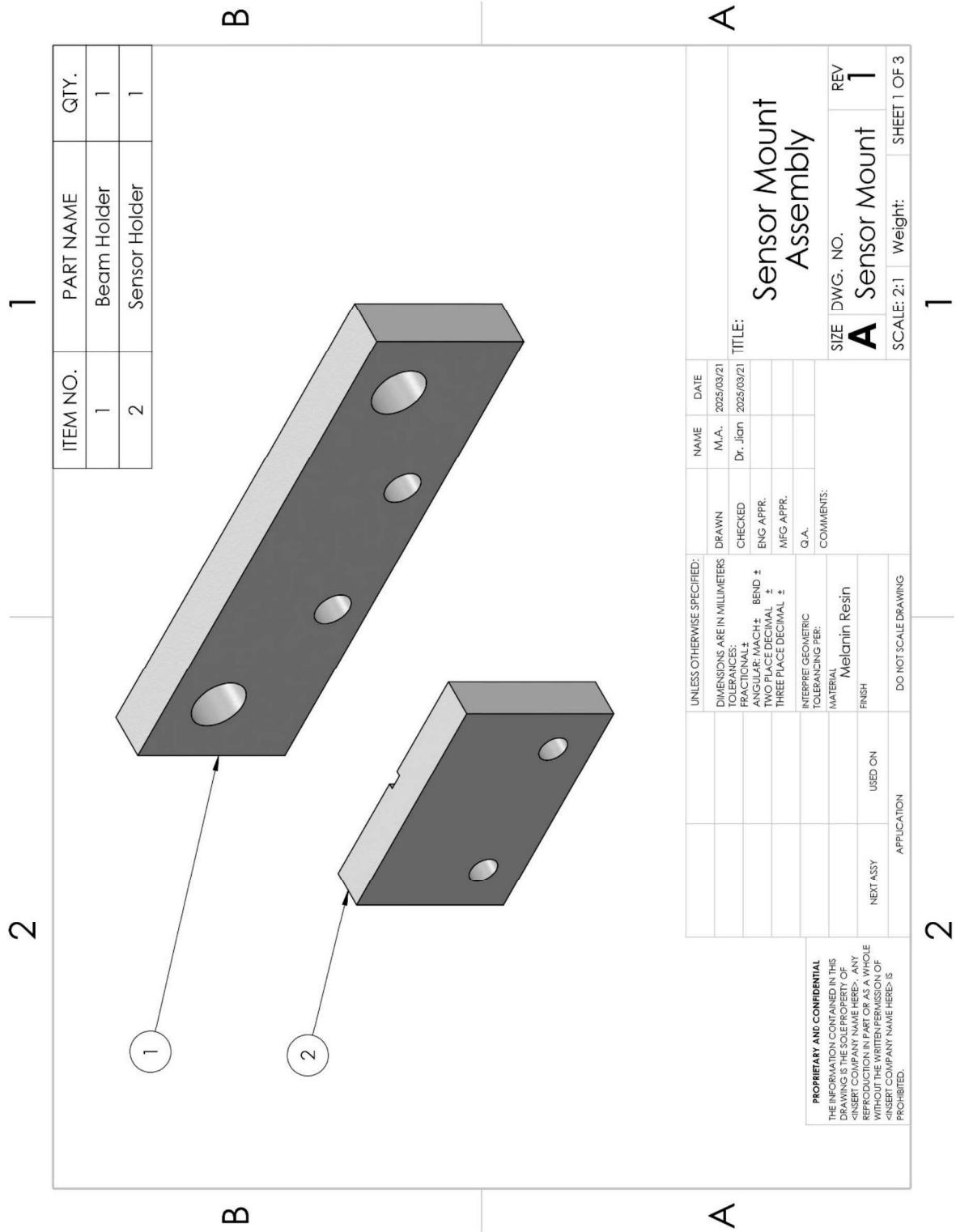


Figure B16. Detailed engineering drawing of 3D printed sensor mount assembly.

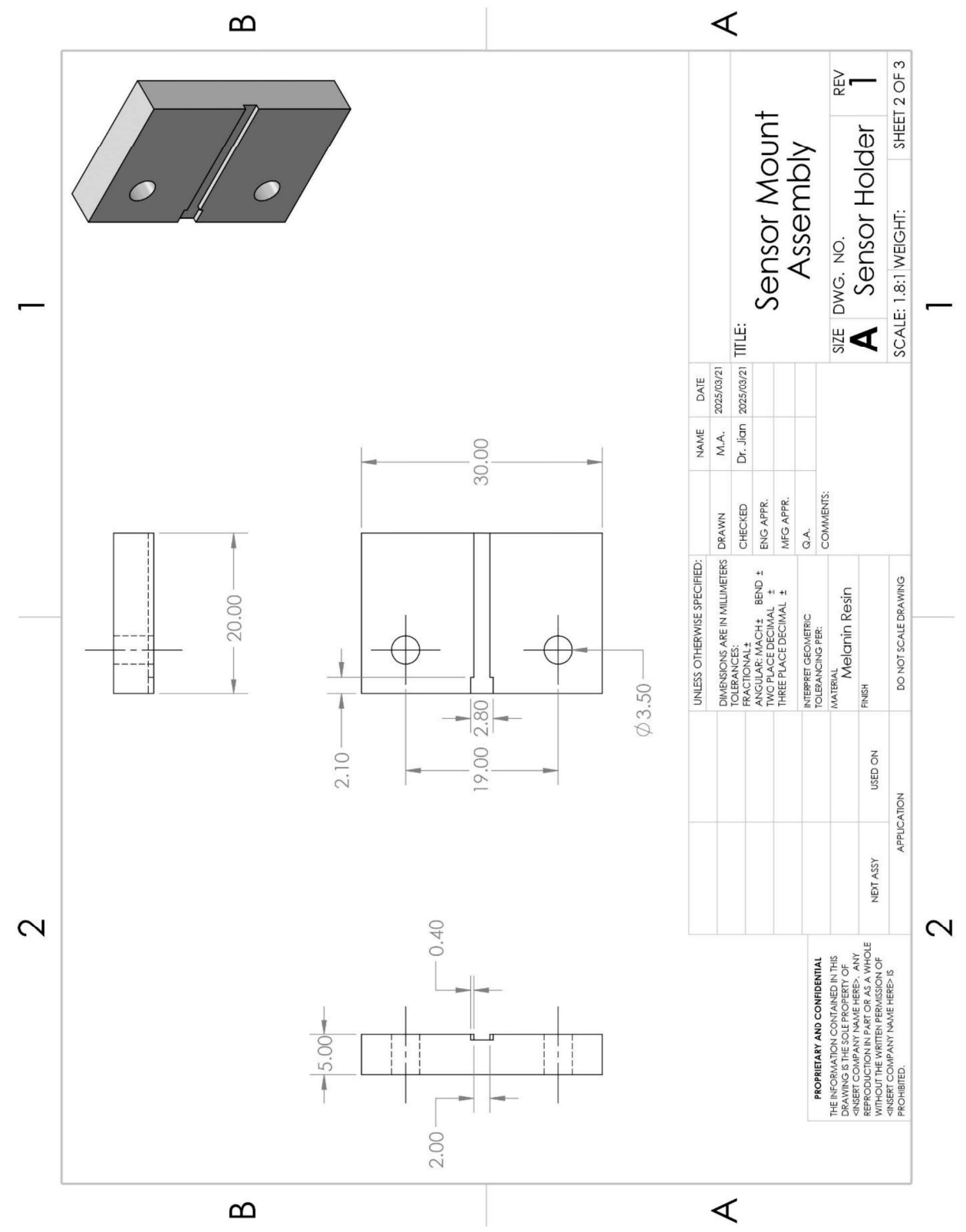


Figure B17. Detailed engineering drawing of 3D printed sensor holder.

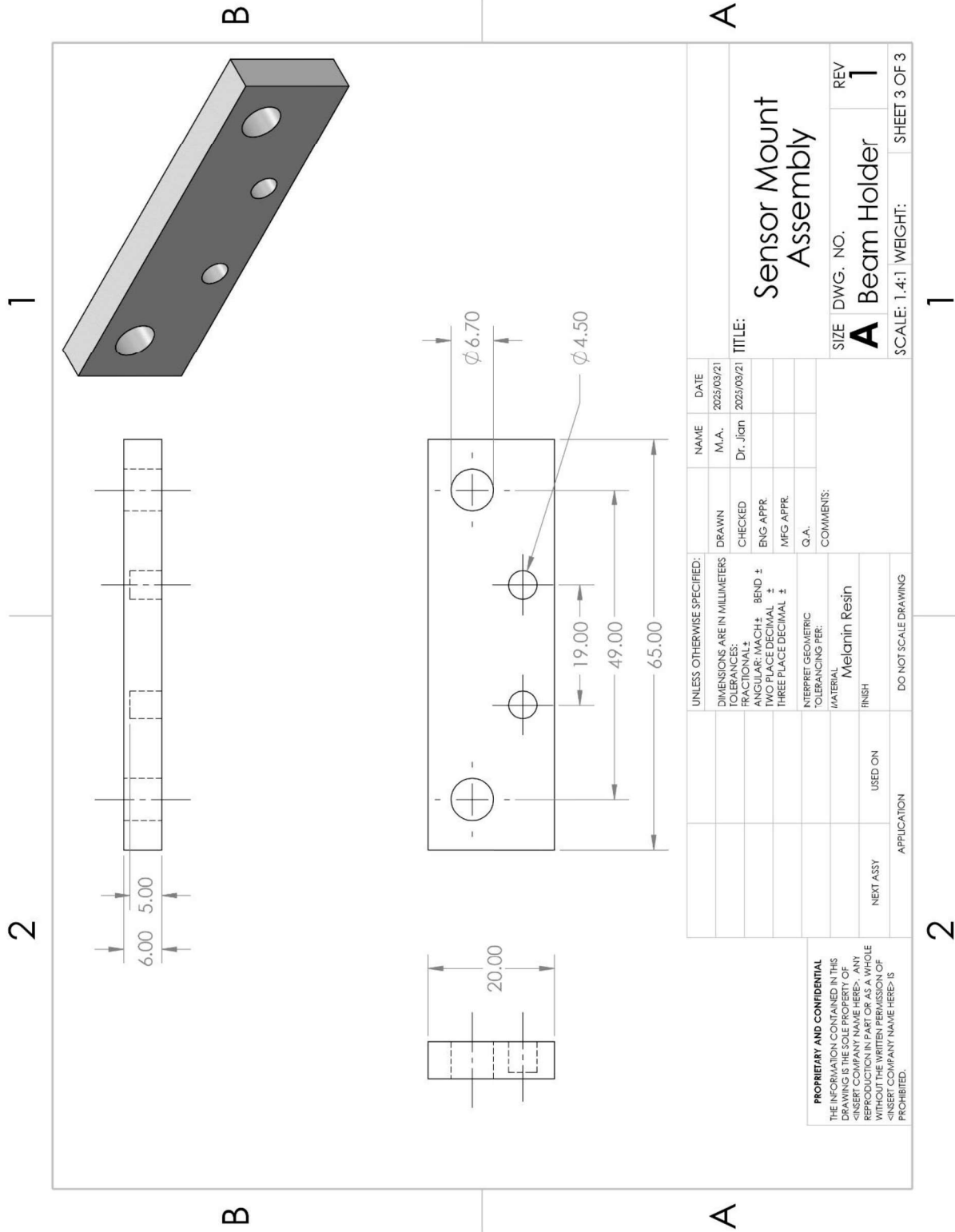


Figure B18. Detailed engineering drawing of 3D printed beam holder.

APPENDIX C: ADDITIONAL INFORMATION ON SELECTED PARTS AND MATERIALS

Appendix C contains additional information on selected parts and materials used in the design.

Perforated Bin Design Calculations and Materials

Vertical and lateral design loads were calculated using the Janssen formula [12]. The equation and calculated loads are shown below.

Janssen Equation

$$\frac{dp}{dz} + \mu * k * \left(\frac{D}{2}\right) * H * P = g * \rho$$

$\frac{dp}{dz}$ = change in pressure with respect to depth

Intermediate (X)

$$X = -4 * \mu * k * \left(\frac{H}{D}\right)$$

Vertical Pressure (σ_z)

$$\sigma_z = \left(\frac{\rho * D * g}{4 * k * \mu}\right) \left(1 - e^{-\frac{4 * k * \mu * z}{D}}\right)$$

z = depth of grain of the bin

Lateral Pressure (σ_x)

$$\sigma_x = k * \sigma_z$$

TABLE C1. RESULTS OBTAINED FROM STRUCTURAL ANALYSIS OF BIN WALL

Parameter	Value
Height (H)	1.524 m
Acceleration due to gravity (g)	9.81 m/s ²
Diameter (D)	1.924 m
Coefficient of friction (μ)	0.25
Vertical Pressure (σ_z)	968.97 Pa (max)
Lateral Pressure (σ_x)	484.48 Pa (max)
Bulk Density (ρ)	770 kg/m ³
Intermediate calculation (X)	-0.40
Lateral vertical ratio [Janssen's constant] (k)	0.5
Lateral Pressure exerted on the Outer column by different of grains	
Canola (5000 Kg)	485 Pa
Wheat (5000 Kg)	388 – 486 Pa

Material properties for the selected perforated sheet metal are included in Table C2. Figure C1 shows the diameter of the perforation, horizontal and vertical distances between the perforations in inches.

TABLE C2. PROPERTIES OF PERFORATED SHEET METAL

Tension Tests	
Yield Strength (min.)	130 MPa
Elongation (min.)	35%
Tensile Strength (min.)	270 MPa
Chemistry and properties of C1008 CR Steel	
Element	Percentage Composition per element
Iron (Fe)	99.00 max
Copper (Cu)	0.20 min
Sulfur (S)	0.00 – 0.05
Manganese (Mn)	0.30 – 0.60
Carbon (C)	0.08 – 0.13
Phosphorus (P)	0.00 – 0.04

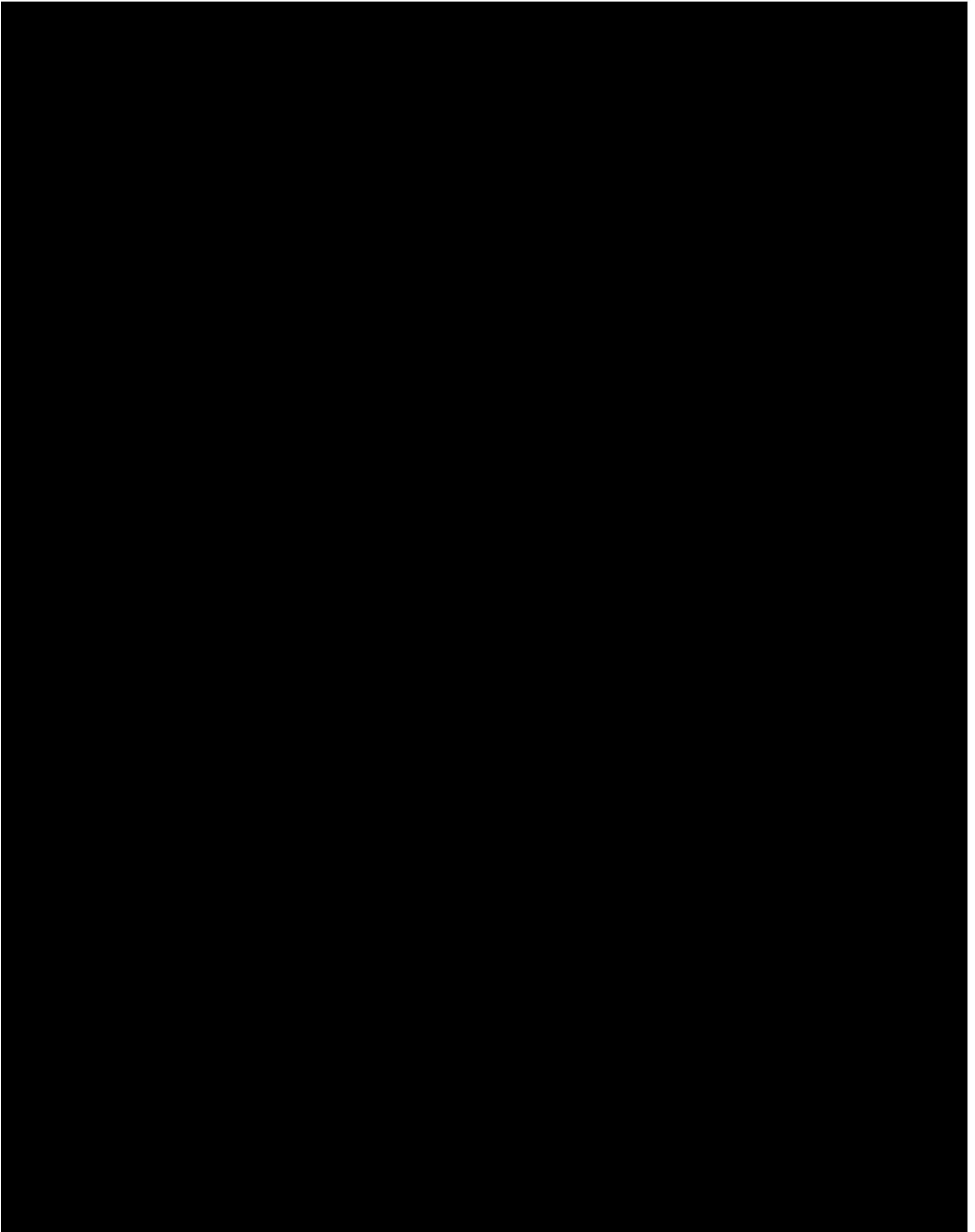


Figure C1. Dimensions of the perforation on the steel sheet metal.

Pitot Tube Support Design Calculations and Materials

Calculations for the 3/8th steel solid square bars used in pitot tube support

Bulk density of wheat (D_w) = 775 kg/m³

Density of steel (D_s) = 7850 kg/m³

Height from the bottom steel bar support to the top of the outer column (H) = 1.8m

Acceleration due to gravity(g) = 9.81 m/sec²

Dimensions of selected steel bar

1. length (L) = 0.51m
2. width (w) = 0.375in = 0.009525m
3. height (h) = 0.375in = 0.009525m

Volume of the square steel bar (V_s)

$$= L * w * h = 0.51 * 0.009525 * 0.009525 = 4.62700687 \times 10^{-5} \text{ m}^3$$

Weight of the square steel bar (W_s)

$$= D_s * V_s * g = 7850 * (4.62700687 \times 10^{-5}) * 9.81 = 3.563188589 \text{ N}$$

Total weight (W_G) of grain acting on the steel bar

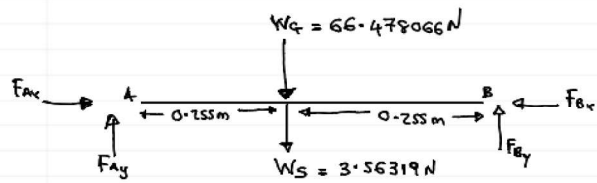
$$= D_w * L * w * h * g = 775 * 0.51 * 0.009525 * 0.009525 = 66.478066 \text{ N}$$

Moment of inertia of steel (I_s)

$$= (w * h^3) / 12 = (0.009525 * 0.009525^3) / 12 = 6.85928253 \times 10^{-5} \text{ m}^4$$

Assumptions made in calculating for the bending moment

- a. square steel bars are welded making it a fixed support



Taking moment about B

$$\sum M_B = 0 \uparrow$$

$$(3.56319 \times 0.255) + (66.478066 \times 0.255) = 0.51 F_{By}$$

$$F_{By} = 35.020592 \text{ N}$$

$$\sum F_y = 0 \uparrow$$

$$F_{Ay} = W_G + W_S - F_{By}$$

$$F_{Ay} = (66.478066 + 3.56319 - 35.020592) \text{ N}$$

$$F_{Ay} = 35.020595 \text{ N}$$

Figure C2. Free body diagram and calculation of forces acting at fixed supports (welded) A and B.

Drawing a shear and moment bending diagram

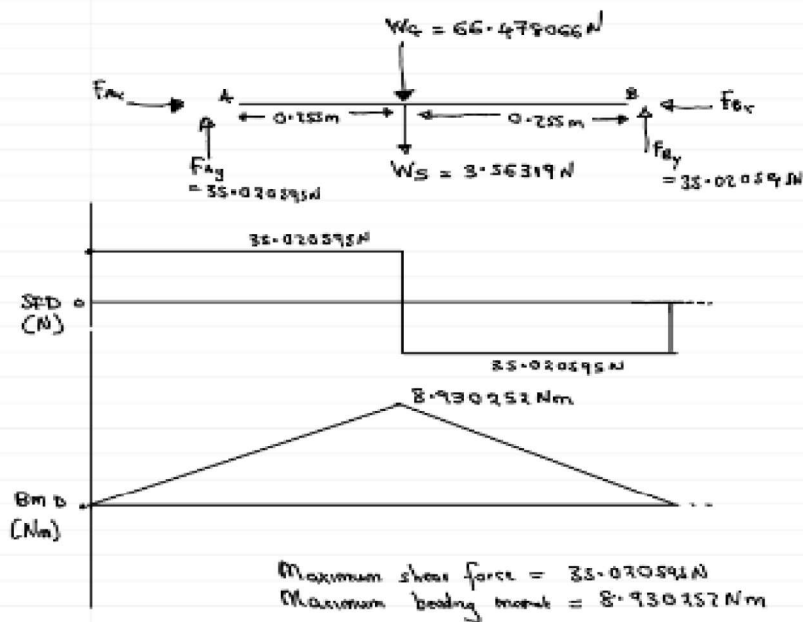


Figure C3. Diagram of the Shear force diagram (SFD) and Bending Moment diagram indicating the maximum shear force and bending moment acting on a 0.375in X 0.375in solid square steel bar.

Maximum shear stress acting on steel bar (V_s) = 35.020595 N

Maximum bending moment (M_B) = 8.930252 Nm

Distance to the neutral axis (a) = 0.004763 m

Maximum Stress acting on the bar (S_{max})

$$= (M_B * a) / (I_s) = (8.930252 * 0.004763) / (6.85928253 \times 10^{-5}) = 620.1055298 \text{ N/m}^2$$

Yield Stress of the material (Y_s) = 248000000 N/m²

Factor of Safety

$$= \text{Yield Stress of the material } (Y_s) / \text{Maximum Stress acting on the bar } (S_{max})$$

$$= (248000000) / (620.1055298) = 3.999.$$

With the factor of safety of 3.999, the solid square steel bar selected and used custom-built metal frame are overdesigned to withstand a vertical pressure exerted by load of grains weighing 66.478N. the solid square metal steel bars of 3/8" were the chosen due to sizes smaller than 3/8" being more difficult to weld.

Fan Specifications

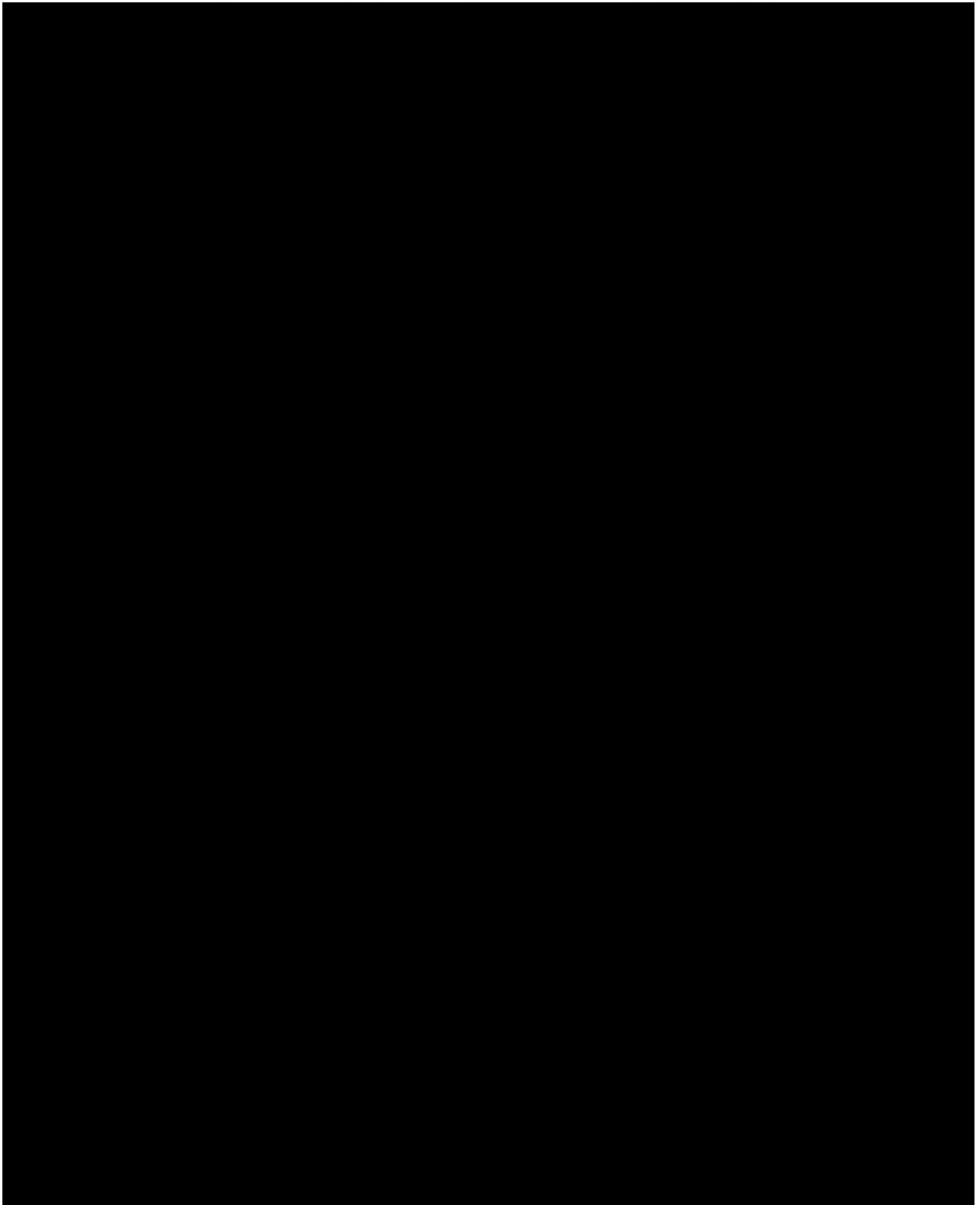


Figure C4. Specifications for Northern Blower fan used for testing.

Mass Flow Sensor Specifications

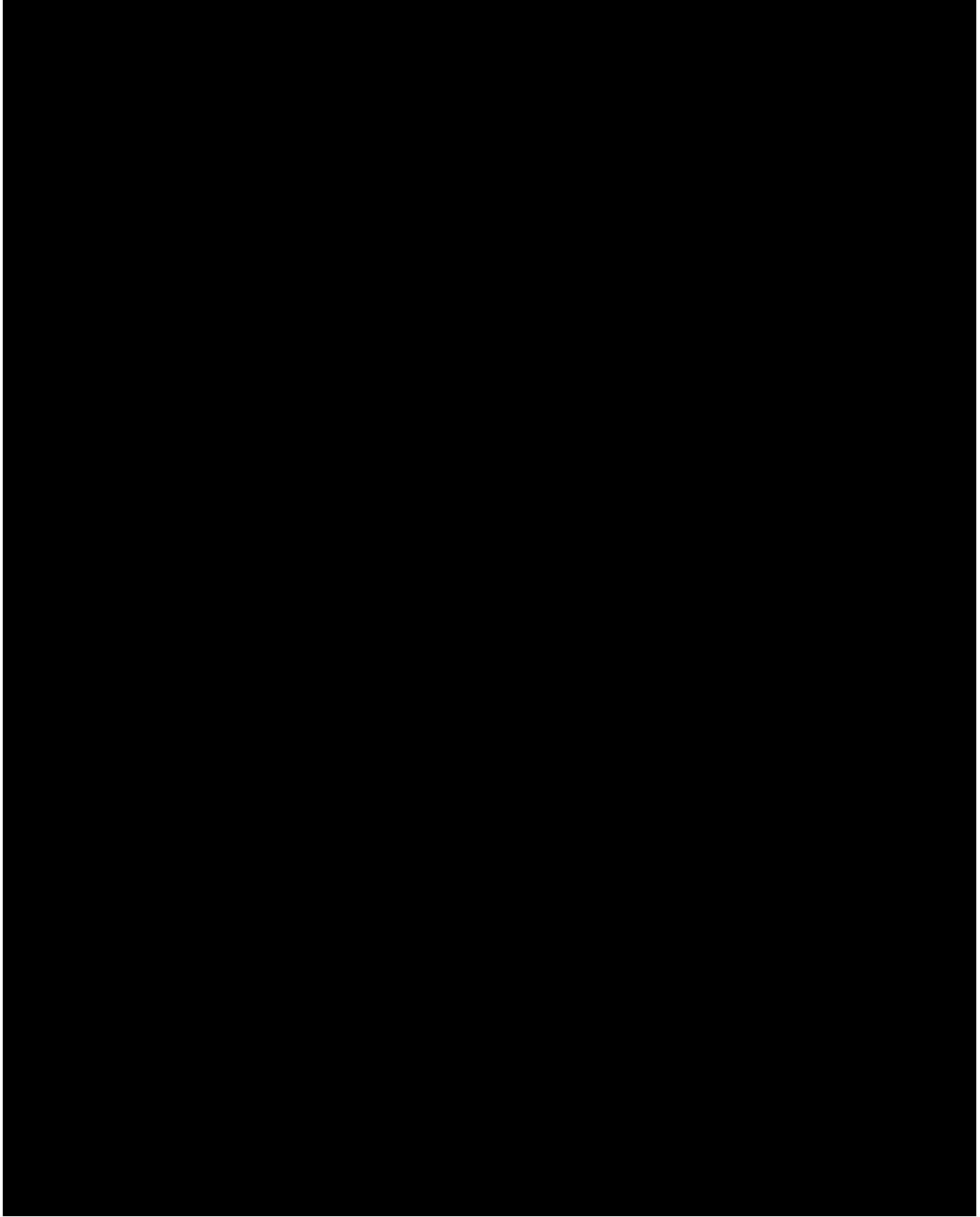


Figure C5. Manufacturer specifications for iST FS7 thermal mass flow sensors [13].

Pitot Tube Specifications

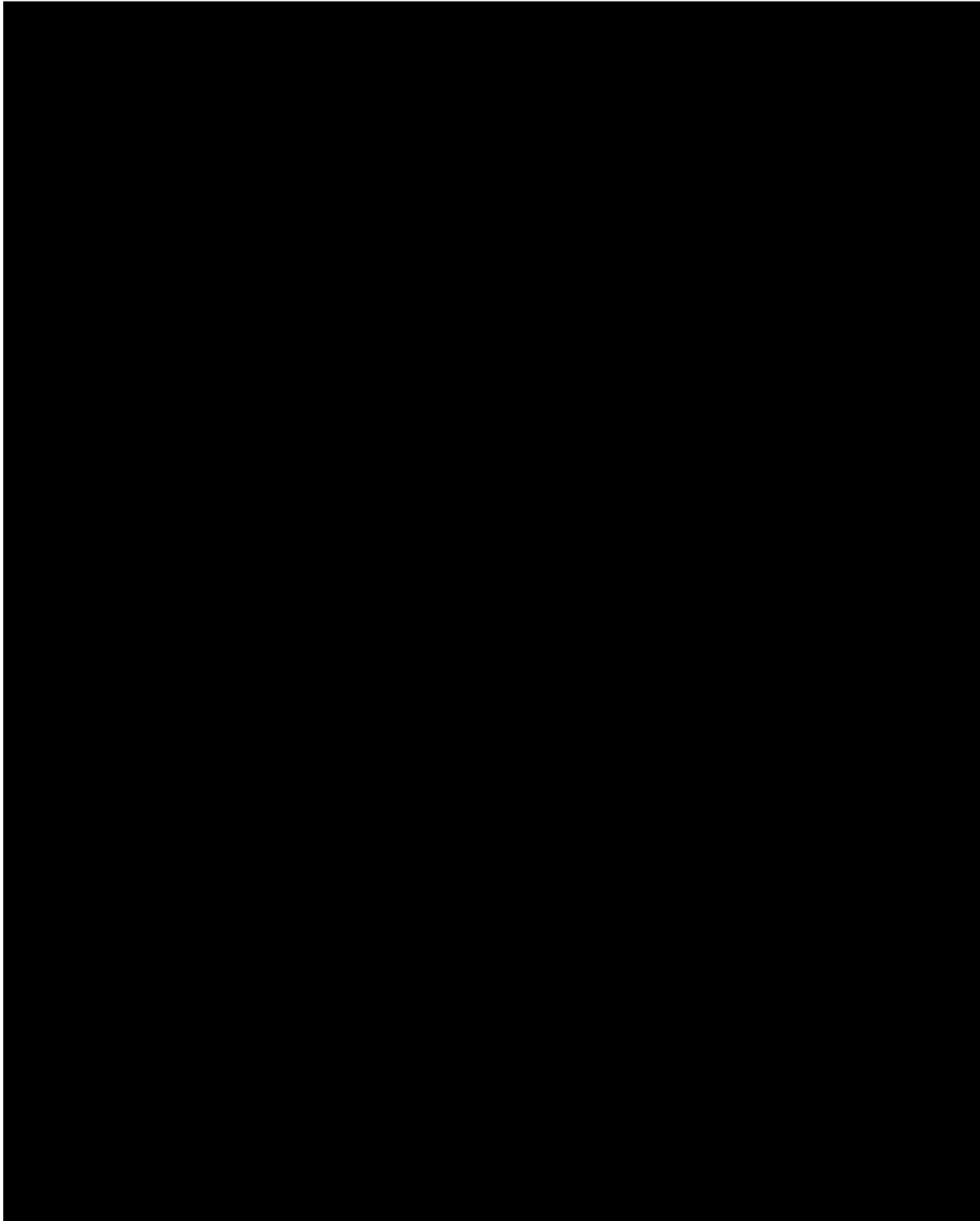


Figure C6. Manufacturer specifications for Dwyer pitot tubes [14].

Hot Wire Anemometer Specifications

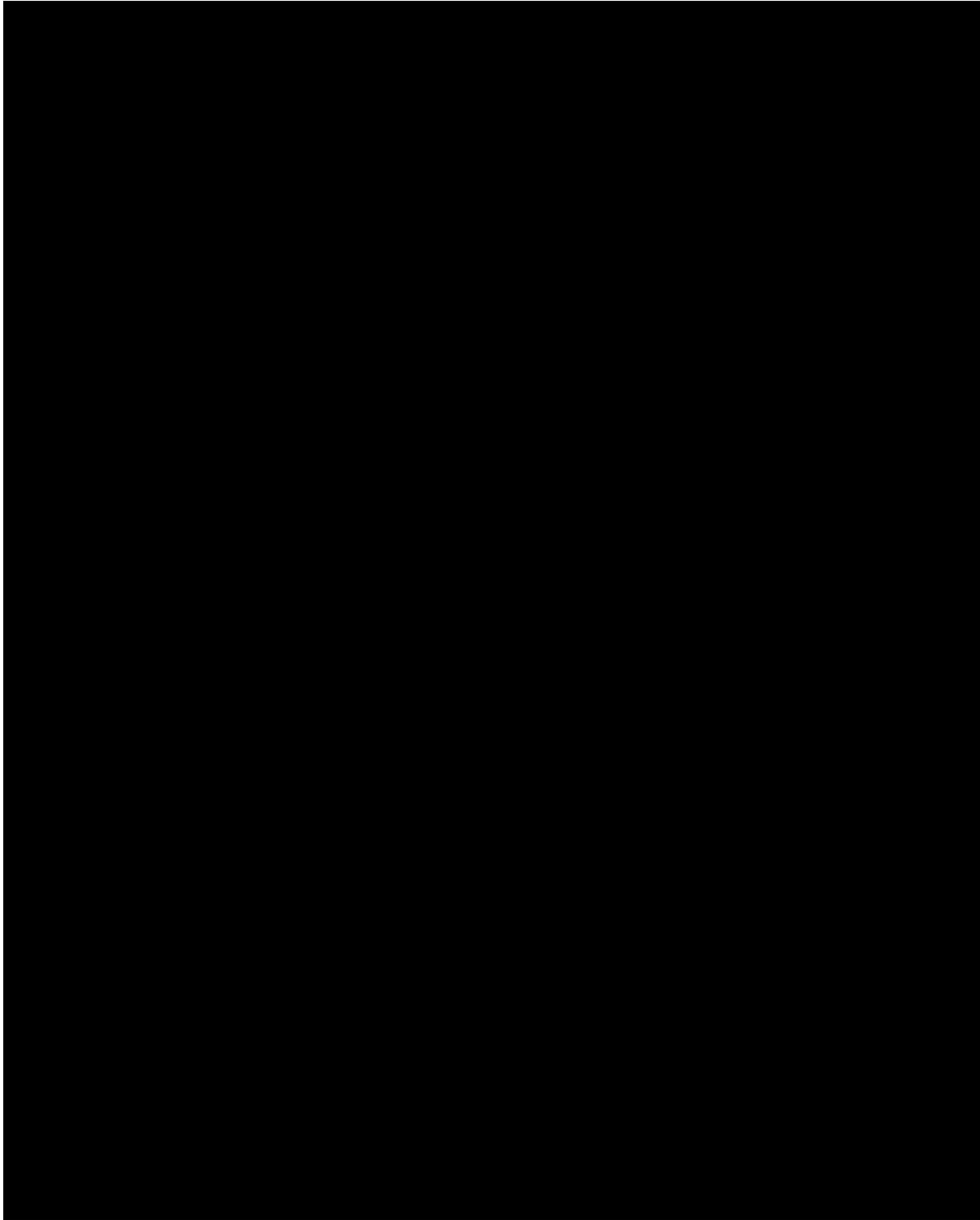


Figure C7. Manufacturer specifications for KANOMAX Anemomaster A031 hot wire anemometer [15].

Digital Manometer Specifications

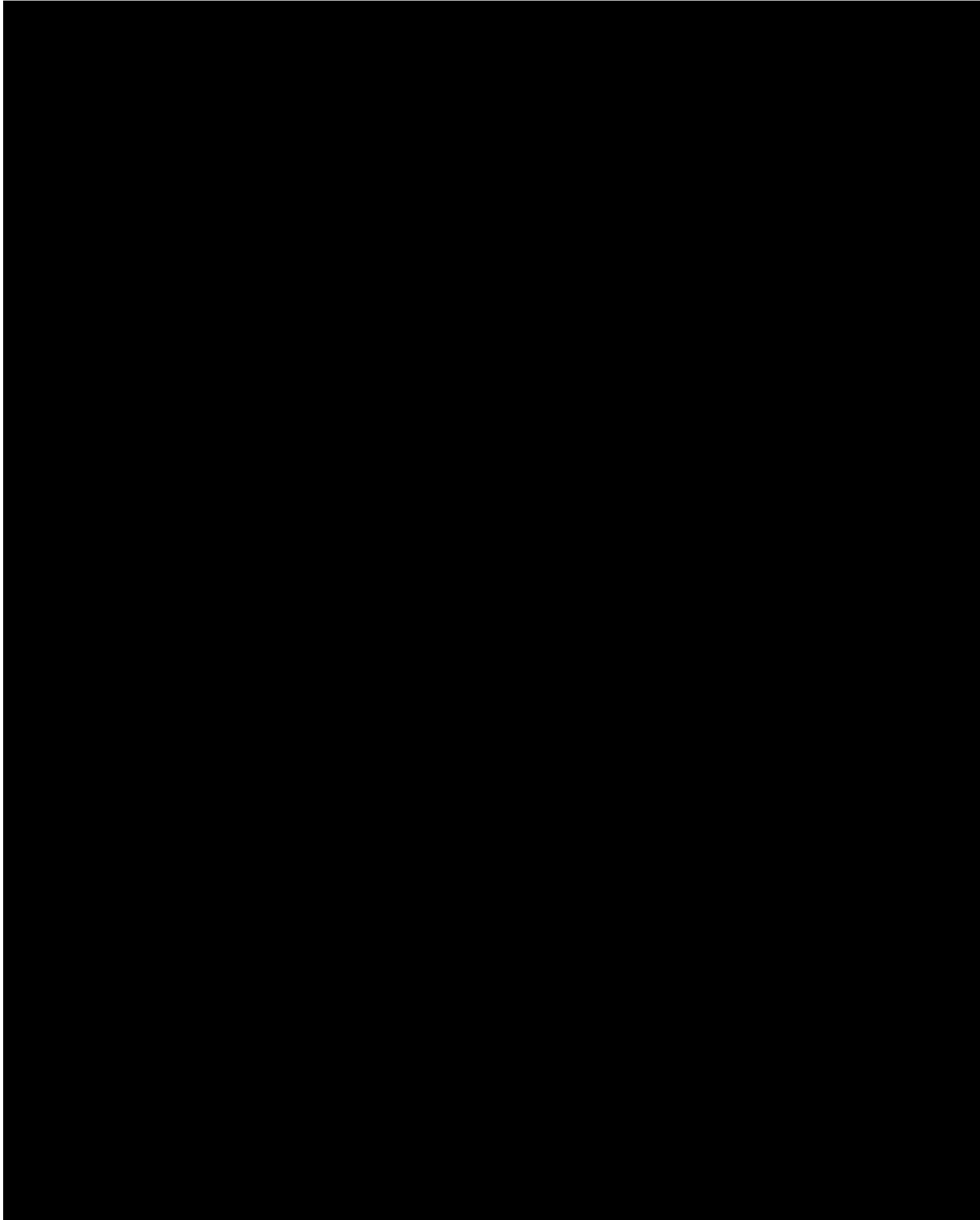


Figure C8. Manufacturer specifications for REED R3030 digital manometer [16].

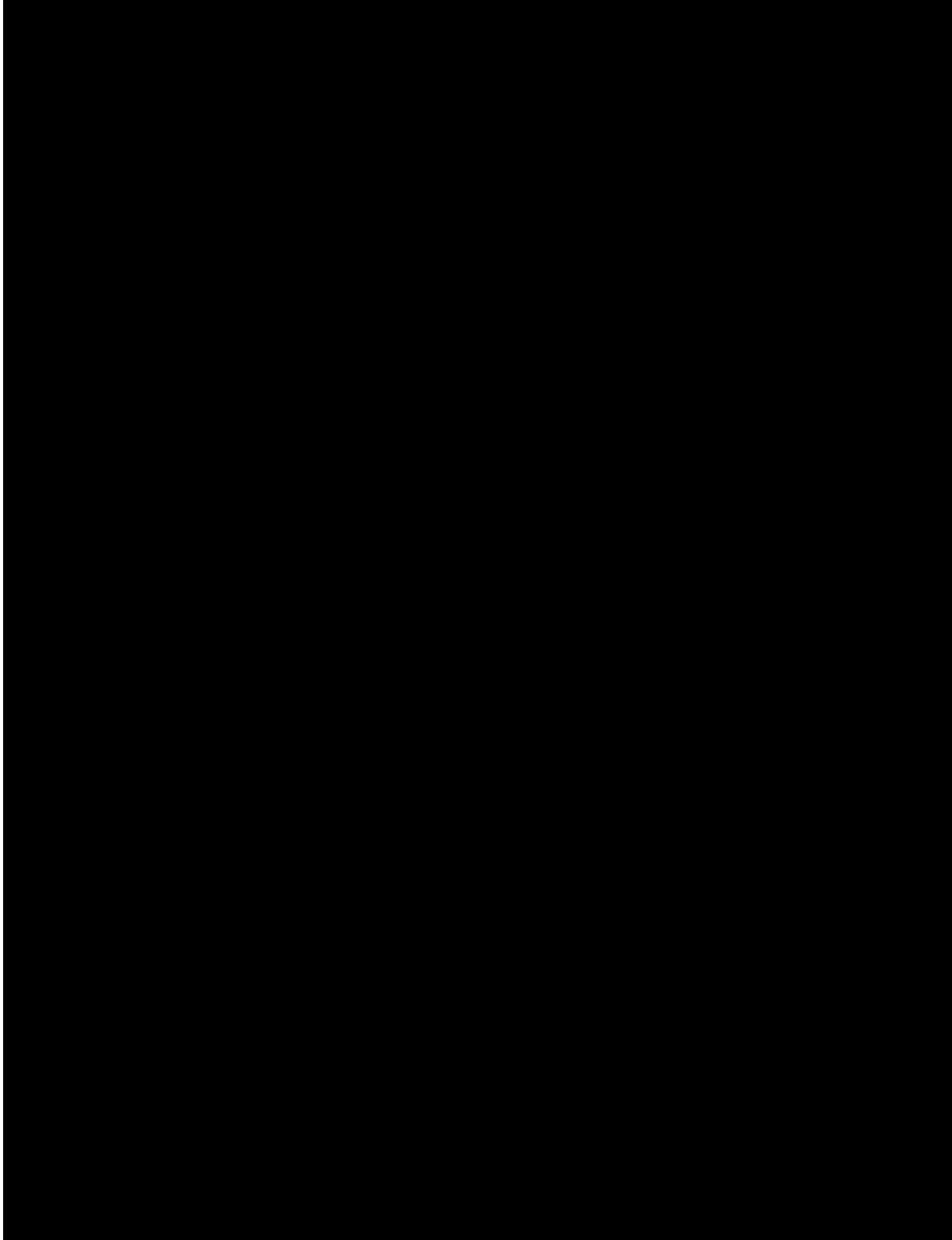


Figure C9. Manufacturer specifications for REED R3030 digital manometer [16].

APPENDIX D: FS7 CALIBRATION CALCULATIONS AND GRAPHS

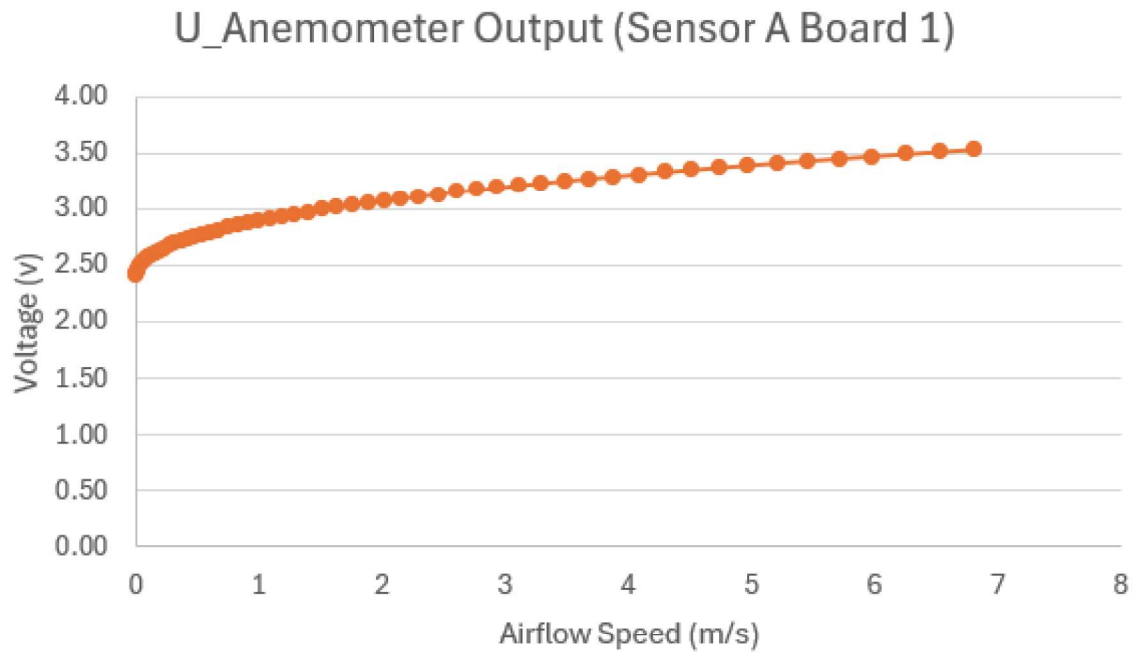
The graphs in the appendix illustrate the relationship between the voltage values measured by the mass flow sensors (A, K, C, L, E, F, G, H, I, and J) and their respective calculated air flow speed values.

$$\vec{v} = \frac{((U - U_0) * (U + U_0))^{\frac{1}{n}}}{\left(k^{\frac{1}{n}}\right) * U_0^{\frac{2}{n}}}$$

The above equation is provided by the mass flow sensor's manual to calculate the air flow's velocity when provided with the corresponding voltage. The parameters n and k are dependent on U0, U50, and U100 which are the voltages at V = 0%, V = 50%, and V = 100% respectively. The parameter n is provided in the manual while k is calculated using the following equation which is also provided by the manual.

$$k = \frac{\left(\frac{U_{50\%}}{U_0}\right)^2 - 1}{\left(\vec{v}_{50\%}\right)^n}$$

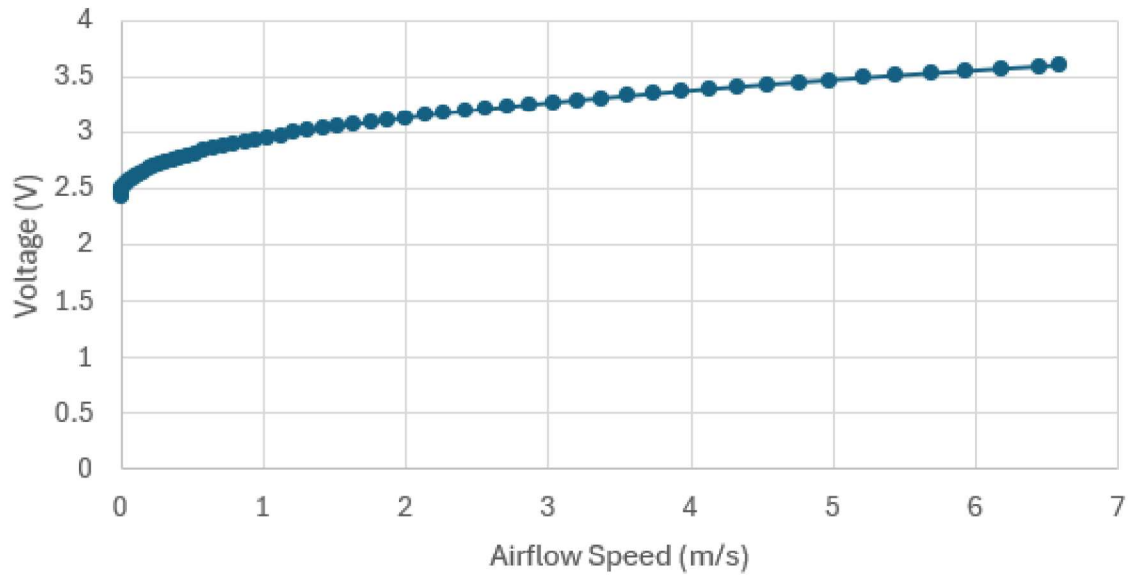
Where $V_{50\%}$ is the airflow speed at 50% of its full strength. As shown in the provided pictures, the equation was divided into smaller parts to prevent errors, and each parameter was calculated and provided separately.



J42				
	A	B	C	D
1	U0	2.41	U50	3.22
2	n	0.5	U100	3.53
3	1/n	2		
4	2/n	4		
5	k	0.439		
6	$k^{(1/n)}$	0.192649851614463		
7	$U0^{(2/n)}$	33.73402561		
8	$k^{(1/n)} * U0^{(2/n)}$	6.498855028		

Figure D1. Calibration graph and calculated parameters for sensor A.

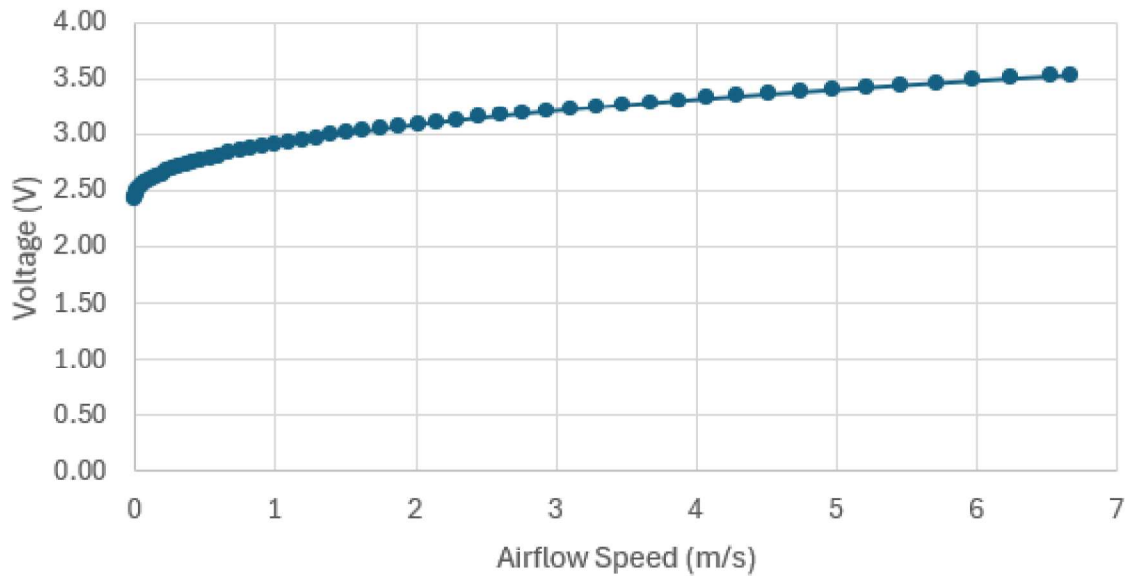
U_Anemometer Output (Sensor K Board 1)



H22				
	A	B	C	D
1	U0	2.43	U50	3.29
2	n	0.5	U100	3.60
3	1/n	2		
4	2/n	4		
5	k	0.466		
6	$k^{(1/n)}$	0.216877194868465		
7	$U0^{(2/n)}$	34.86784401		
8	$k^{(1/n)} * U0^{(2/n)}$	7.5620402		

Figure D2. Calibration graph and calculated parameters for sensor K.

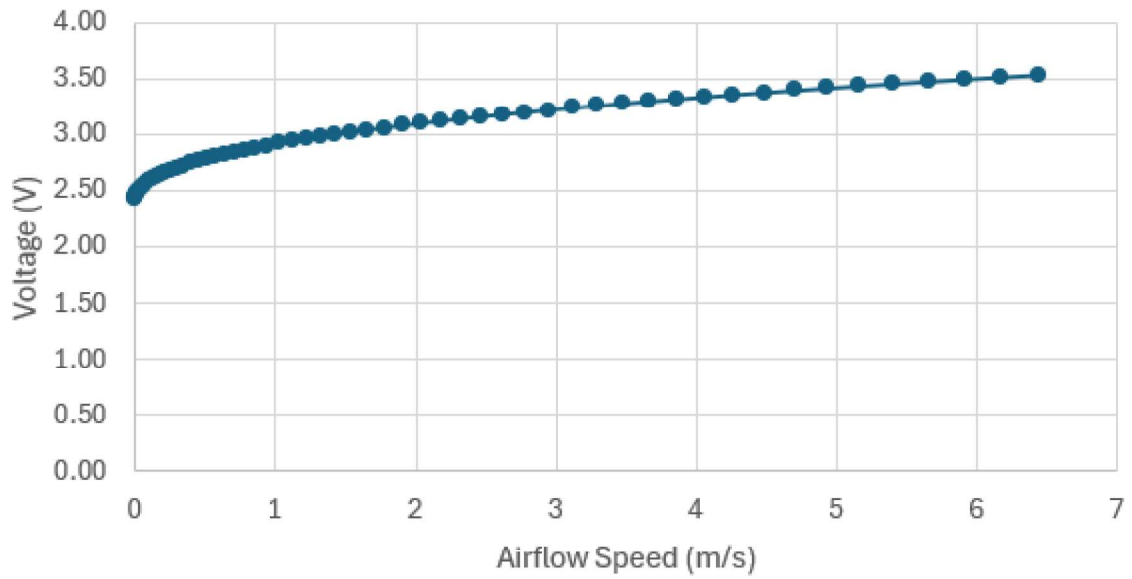
U_Anemometer Output (Sensor C Board 1)



J1				
	A	B	C	D
1	U0	2.43	U50	3.24
2	n	0.5	U100	3.54
3	1/n	2		
4	2/n	4		
5	k	0.435		
6	$k^{(1/n)}$	0.189043209876543		
7	$U0^{(2/n)}$	34.86784401		
8	$k^{(1/n)} * U0^{(2/n)}$	6.591529153		

Figure D3. Calibration graph and calculated parameters for sensor C.

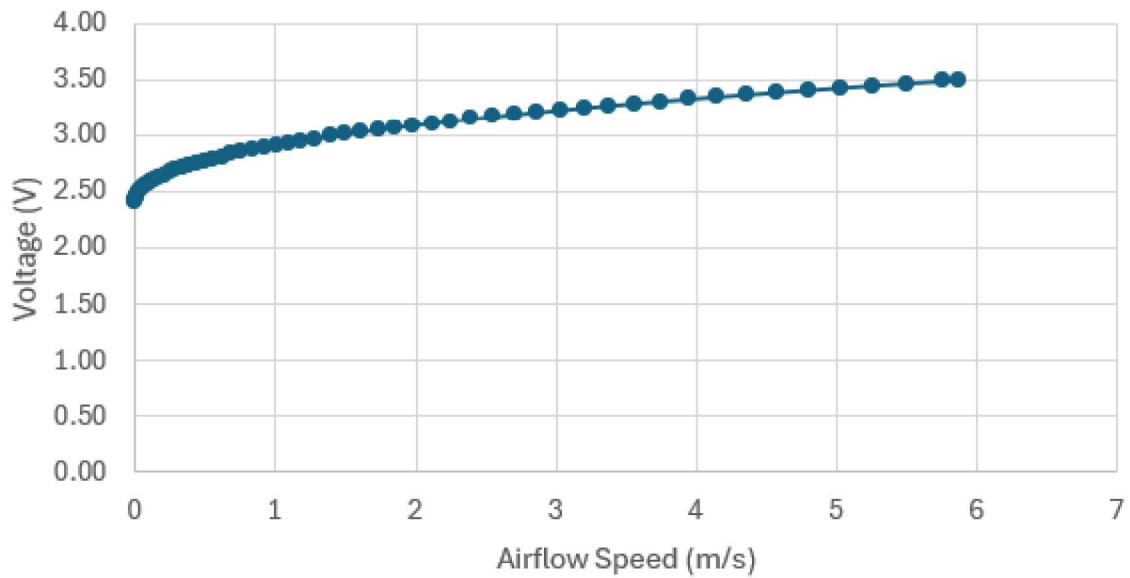
U_Anemometer Output (Sensor L Board 1)



N9				
	A	B	C	D
1	U0	2.42	U50	3.25
2	n	0.5	U100	3.54
3	1/n	2		
4	2/n	4		
5	k	0.449		
6	k^(1/n)	0.201795213295974		
7	U0^(2/n)	34.29742096		
8	k^(1/n)*U0^(2/n)	6.921055378		

Figure D4. Calibration graph and calculated parameters for sensor L.

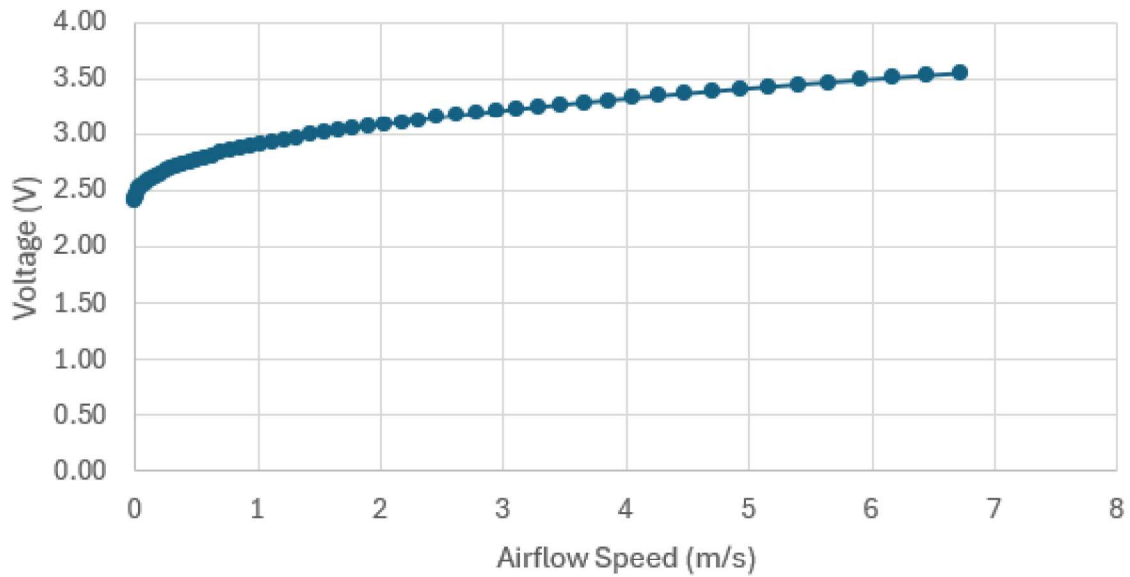
U_Anemometer Output (Sensor E Board 1)



O14				
	A	B	C	D
1	U0	2.41	U50	3.25
2	n	0.5	U100	3.50
3	1/n	2		
4	2/n	4		
5	k	0.458		
6	$k^{(1/n)}$	0.209398364774645		
7	$U0^{(2/n)}$	33.73402561		
8	$k^{(1/n)} * U0^{(2/n)}$	7.0638498		

Figure D5. Calibration graph and calculated parameters for sensor E.

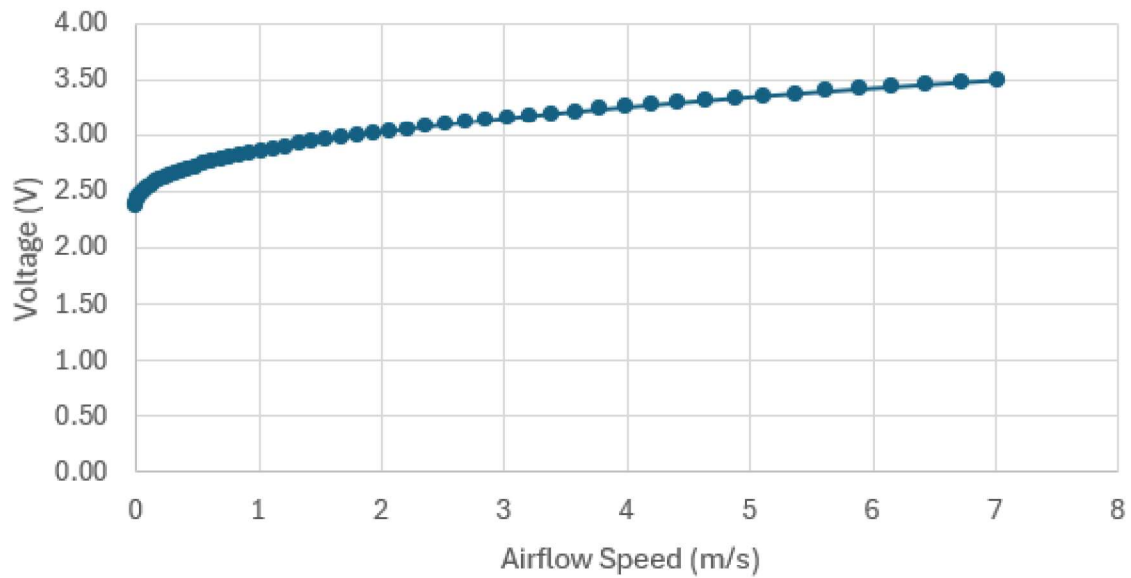
U_Anemometer Output (Sensor F Board 2)



Q14				
	A	B	C	D
1	U0	2.41	U50	3.24
2	n	0.5	U100	3.55
3	1/n	2		
4	2/n	4		
5	k	0.451		
6	$k^{(1/n)}$	0.203720593046796		
7	$U0^{(2/n)}$	33.73402561		
8	$k^{(1/n)} * U0^{(2/n)}$	6.872315703		

Figure D6. Calibration graph and calculated parameters for sensor F.

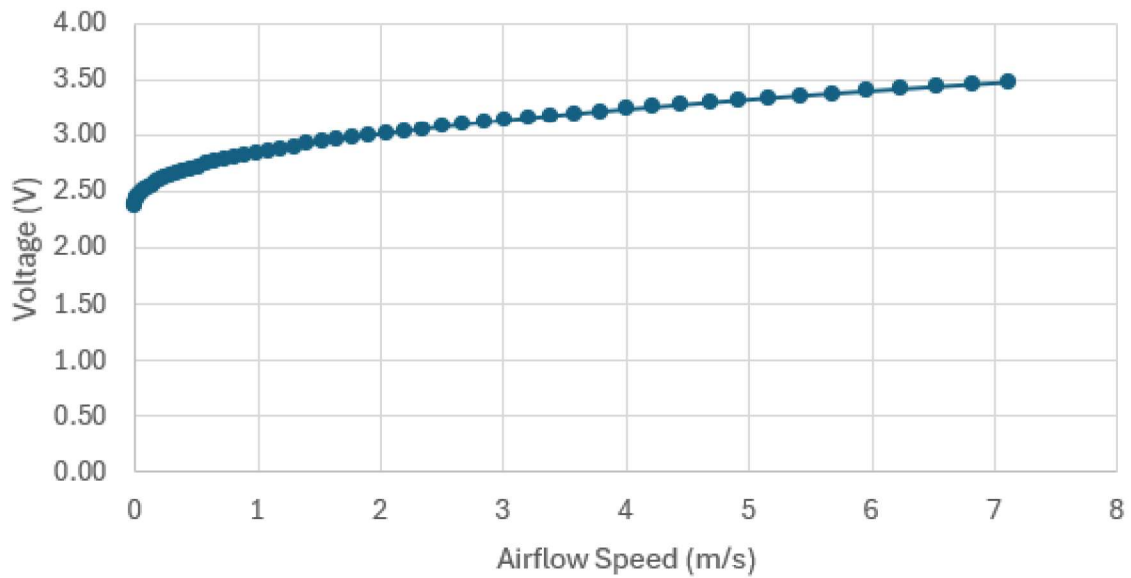
U_Anemometer Output (Sensor G Board 2)



M23				
	A	B	C	D
1	U0	2.38	U50	3.18
2	n	0.5	U100	3.50
3	1/n	2		
4	2/n	4		
5	k	0.439		
6	$k^{(1/n)}$	0.192695578919040		
7	$U0^{(2/n)}$	32.08542736		
8	$k^{(1/n)} * U0^{(2/n)}$	6.18272		

Figure D7. Calibration graph and calculated parameters for sensor G.

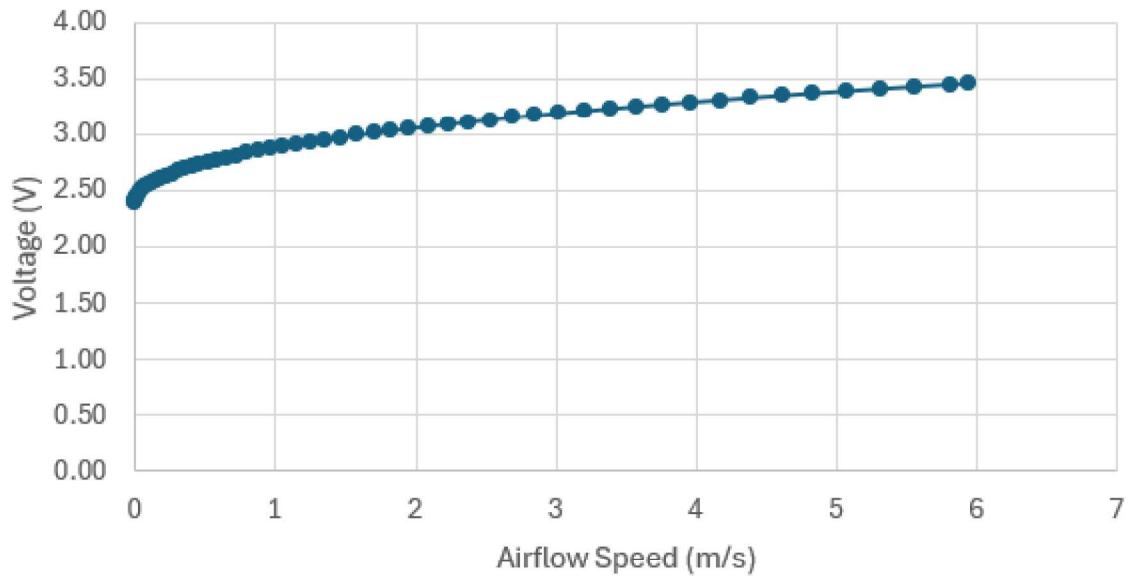
U_Anemometer Output (Sensor H Board 2)



Q12				
	A	B	C	D
1	U0	2.38	U50	3.16
2	n	0.5	U100	3.48
3	1/n	2		
4	2/n	4		
5	k	0.426		
6	$k^{(1/n)}$	0.181865754335398		
7	$U0^{(2/n)}$	32.08542736		
8	$k^{(1/n)} * U0^{(2/n)}$	5.83524045		

Figure D8. Calibration graph and calculated parameters for sensor H.

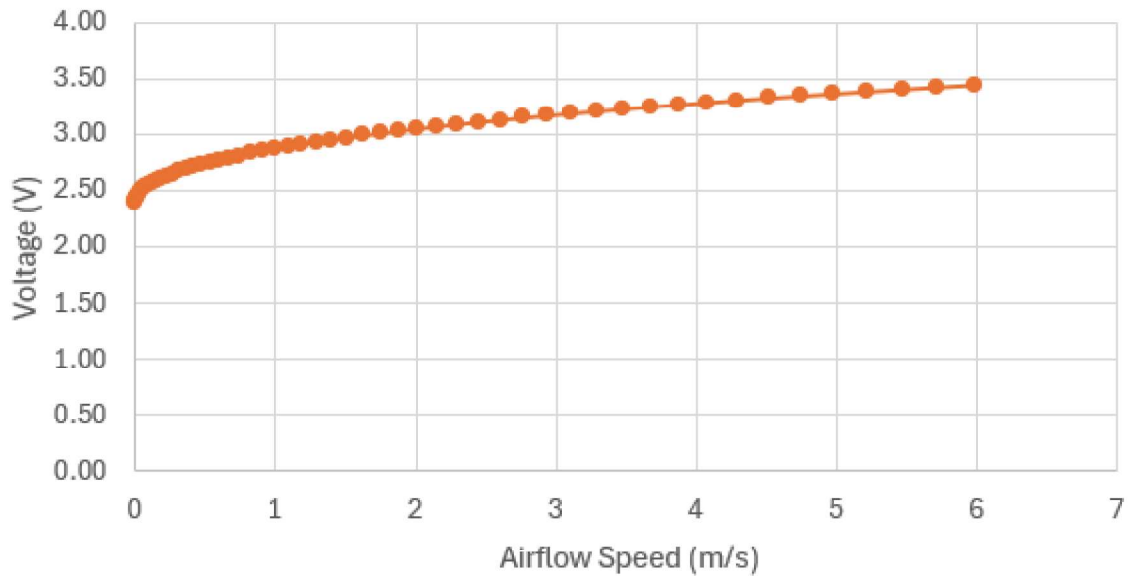
U_Anemometer Output (Sensor I Board 2)



R10				
	A	B	C	D
1	U0	2.39	U50	3.21
2	n	0.5	U100	3.46
3	1/n	2		
4	2/n	4		
5	k	0.449		
6	$k^{(1/n)}$	0.201958518719026		
7	$U0^{(2/n)}$	32.62808641		
8	$k^{(1/n)} * U0^{(2/n)}$	6.58952		

Figure D9. Calibration graph and calculated parameters for sensor I.

U_Anemometer Output (Sensor J Board 2)



H21					
	A	B	C	D	
1	U0	2.39	U50	3.20	
2	n	0.5	U100	3.44	
3	1/n	2			
4	2/n	4			
5	k	0.443			
6	$k^{(1/n)}$	0.196359569562786			
7	$U0^{(2/n)}$	32.62808641			
8	$k^{(1/n)} * U0^{(2/n)}$	6.406837003			

Figure D10. Calibration graph and calculated parameters for sensor J.